Achieving long-term stability of thin-film electrodes for neurostimulation

Poppy Oldroyd [1,2] *George Malliaras* [1, *]

[1] Electrical Engineering Division, Department of Engineering, University of Cambridge, 9 JJ Thomson Avenue, CB3 0FA, United Kingdom

[2] Email: pjo38@cam.ac.uk

* Corresponding author: Email: gm603@cam.ac.uk , Telephone number: +44 (0)1223 748312

Abstract

Implantable electrodes that can reliably measure brain activity and deliver an electrical stimulus to a target tissue are increasingly employed to treat various neurological diseases and neuropsychiatric disorders. Flexible thin-film electrodes have gained attention over the past few years to minimise invasiveness and damage upon implantation. Research has previously focused on optimising the electrode's electrical and mechanical properties; however, their chronic stability must be validated to translate electrodes from a research to a clinical application. Neurostimulation electrodes, which actively inject charge, have yet to reliably demonstrate continuous functionality for ten years or more *in vivo*, the accepted metric for clinical viability. Long-term stability can only be achieved if the focus switches to investigating how and why such devices fail. Unfortunately, there is a field-wide reluctance to investigate device stability and failures, which hinders device optimisation. This review surveys thin-film electrode designs with a focus on adhesion between electrode layers and the interactions with the surrounding environment. A comprehensive summary of the abiotic failure modes faced by such electrodes is presented, and to encourage investigation, systematic methods for analysing their origin are recommended. Finally, approaches to reducing the likelihood of device failure are offered.

Keywords: (bioelectronics, neurostimulation, thin-film electrodes, chronic stability)

1. Introduction

Implantable electrodes that can deliver an electrical stimulus to the brain have shown promise in addressing various neurological diseases and neuropsychiatric disorders [1]. Previous research has demonstrated their clinical potential in treating Parkinson's disease [2], suppression of epileptic seizures [3], and managing illnesses such as treatment-resistant depression [4,5] (Figure 1). Often referred to as "electroceuticals", the modulation of the immune response with electrical pulses, have also been used to treat Crohn's disease [6], obsessive-compulsive disorder [7], and obesity [8].

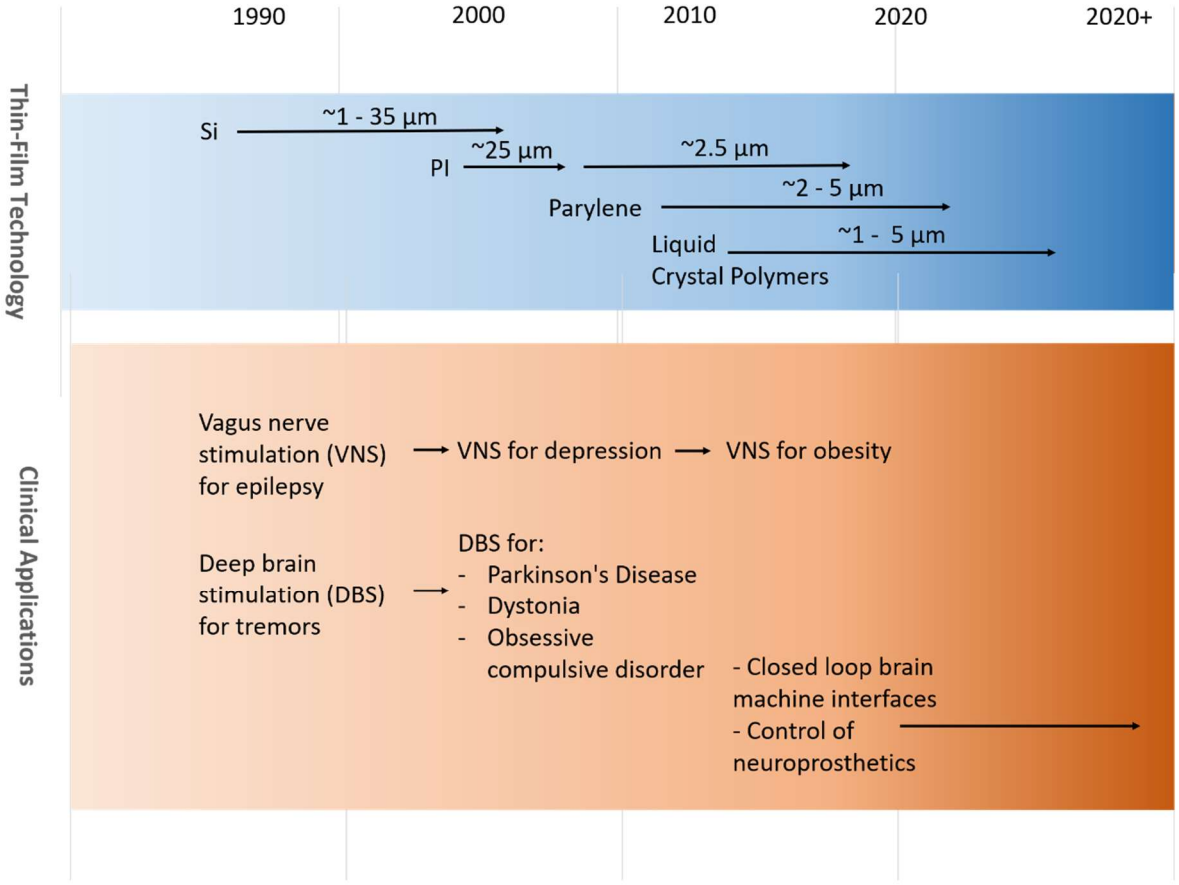

Figure 1: Chronological development of representative technology for thin-film electrodes and the parellel development of their clinical applications.

Implantable electrodes used for neuromodulation have improved dramatically over the last four decades (Figure 1). Electrodes have evolved from thick, hand-made pieces of metal which protruded out of the skull into thin layers of micromachined metal foils implanted under the dura [9]. During this evolution, there was also a paradigm shift in industry to thin-film fabrication. Thin-films semi-

conductors demonstrated better spatial resolution, novel form factors (flexible and stretchable), higher reproducibility, and higher throughput. As a result of these desirable properties, electrodes fabricated from thin-films have gained attention over the past few decades for their use in neuromodulation [10–16]. These electrodes are composed of micro-fabricated thin stacks of substrate (<10 μm), metal electrodes (<100 nm), and insulation layers (<10 μm). These thin layers produce conformable, flexible electrodes suitable for neural interfacing [10,17]. This surge in thin-film technology addresses the growing need for highly selective and high-density microelectrode arrays, enabling precise stimulation and recording of single neurons [18]. To translate electrodes from a research to a clinical application, the electrodes must demonstrate long-term safety and efficacy in pre-clinical evaluations; both properties require stability of the electrode [19,20]. Due to the electrodes' thin nature, thick-film physics and modelling cannot be directly applied [21]. Smaller electrodes result in more significant edge effects, have higher impedance, and require a higher current density meaning the electrode is under more stress and danger of electromigration. To complicate matters further, electrodes need to be thin enough to remain flexible while maintaining mechanical stability upon implantation. As a result, the electrode design is crucial, providing the physical interface between the biological neural tissue and the implanted electronics [22]; this has led to a plethora of new materials being developed for electrode fabrication [23,24].

The biological environment into which the electrodes are inserted is harsh and is exacerbated by inflammatory reactions upon implantation [25]; electrodes must be resilient to corrosion, delamination, swelling, dissolution, and mechanical strain, all while under continuous electrical stimulation [26]. A successful neurostimulation device will demonstrate, among other things, biocompatibility, mechanical stability on insertion, and electrical stability upon stimulation [26]. Fabricating a device that meets the above criteria has proven challenging, with device failure often representing the most frequent complication in neural implant surgeries [27].

The failure of thin-film electrodes can be separated broadly into two modes: (1) intrinsic failure of the device and (2) failure due to changes in the environment such as scar tissue formation, neural death, and loss of contact between the electrode and target tissue [28] (Figure 2). Both failure modes limit chronic recording and stimulation ability, inhibit their clinical translation, and adversely affect patients [29,30]. Reducing the likelihood of these failure modes is one of the most critical challenges currently faced in neural interface engineering. This review focuses on the first and often neglected of these failure modes: the intrinsic failure of the device. For device failure due to changes in the electrode environment and foreign body reaction, the reader is directed to several excellent reviews [25,31–34].

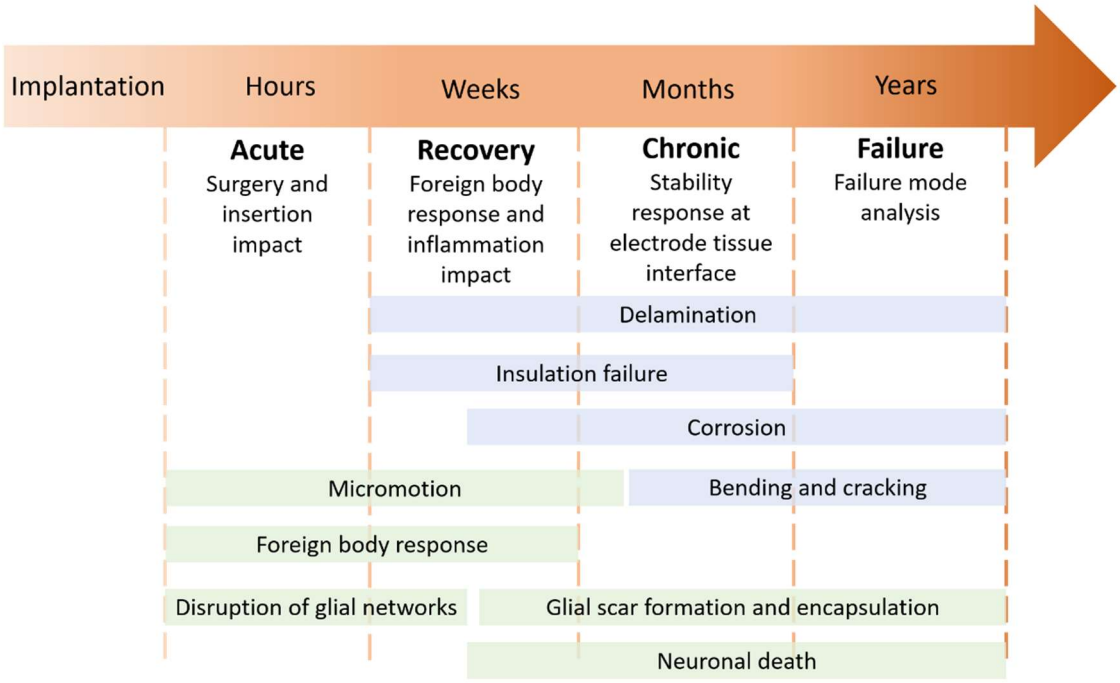

Figure 2: Key time points in the investigation of the stability of chronic thin-film stimulation electrodes. Failure modes have been identified as biotic in green (referring to biological failures) or abiotic in blue (referring to engineering failures).

2. Chronic Studies

In the order of weeks and months, chronic stability has been reported for recording devices [35–37]. For stimulation devices, the reported stability is considerably less [16,38,39]. However, to be clinically viable, the devices need to consistently demonstrate continuous functionality for ten years or more *in vivo*, a metric that has not yet been achieved [40]. Long-term reliability and stability of the device are also crucial for neuroscience applications such as the investigation of brain diseases,

application of deep brain stimulation, and treatment of Parkinson's disease which rely heavily on chronic studies [41].

There are plenty of studies on pre-clinical assessments in animal models [42–44] and intraoperative monitoring in acute clinical trials [45–48], but investigation into the long-term stability of these electrodes is often neglected with a consistent lack of device assessment and electrode stability evaluation post explanation. Microscopy and histology analysis of the explanted electrodes can give insight into the device performance and the effect of chronic stimulation on the device. While some groups have begun investigations into device failures [49–52], this research is scarce (Figure 3). Long-term studies into device stability and failure are hard to fund, challenging to perform, and tough to publish; these barriers hinder the advancement of the field. From the few pre-clinical studies available, when device failures are reported there is a consistent lack of investigation into why, with failures simply reported as "high impedance" [53] or "electrode breakage" [54].

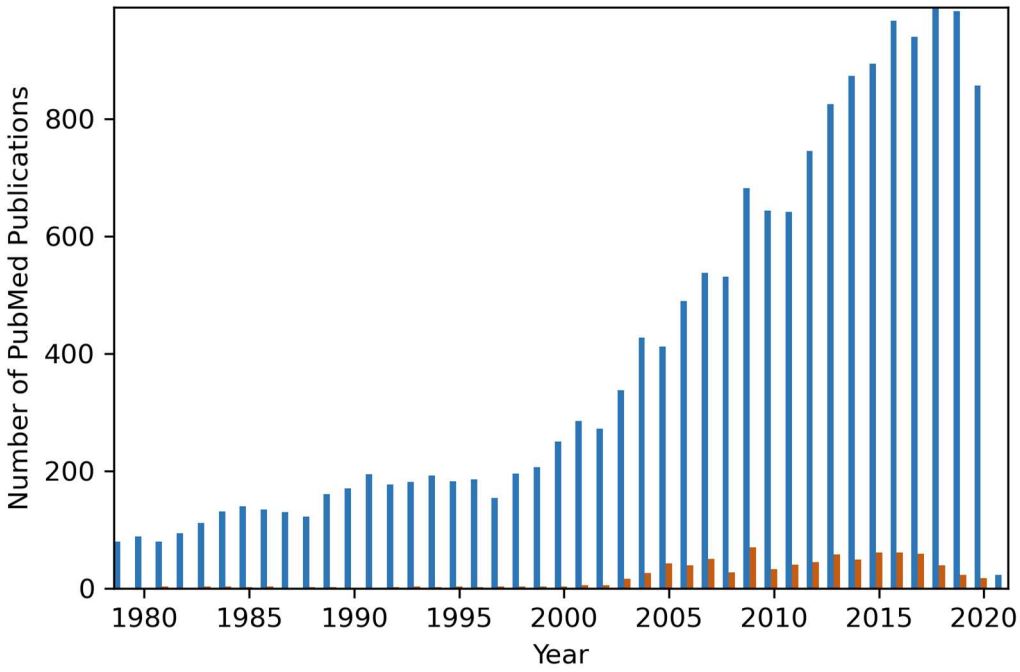

Figure 3: Number of PubMed publications 1976-2020 inclusive. Orange represents results using the search criteria: "Neural" AND "Electrodes" AND "Failure"; Blue represents results using the search criteria: "Neural" AND "Electrodes".

A universal dilemma in clinical testing of devices is choosing the appropriate duration of the animal and human studies. Electrode failure is an often neglected avenue of inquiry because studies tend to run for pre-determined timescales rather than until device failure, which inhibits the investigation of failure modes (Table 1). While the FDA has accepted pre-clinical study lengths of 3 to 6 months, ideally, experiments should be run for longer timescales. Despite the initial requirement for more resources, this will result in fewer devices failure in the long-term.

Author	Electrode Design		*In vitro* testing		*In vivo* testing				Failure observations
	Sub., Elec., Ins, Coat.	Design	Assessment tools	Stimulation duration (weeks)	Type, implant location	Assessment tools	Stimulation duration (weeks)	Reason for termination	
Dalrymple [55]	Si, Pt-Ir, Si, CH	Wire	EIS, CV	5	Rat, Cochlear	EIS, CV	5	E	Delamination of CH coating
Lago [56]	Teflon, Pt-Ir, Teflon, n/a	Wire	n/a	n/a	Rat, Sciatic nerve	AP	13	E	Impedance increase
Weiland [16]	Si, Au, Si, n/a	Pitchfork array	EIS, CV	<1	Guinea pig, cortex	EIS, CV	2	E	Reduced CIC Organic film formation
Donaldson [57]	Si, Pt-Ir, Si, n/a	Wire	SEM	2	Human, Anterior root, leg, retina	SEM	25-150 hours	E	Metal removal and redeposition
Shepherd [58]	Silastic, Pt, Silastic, n/a	Wire	n/a	n/a	Human, scala tympani	SEM, EIS	140	E	Localised hole formation
George [51]	Si, Pt, Si (Utah), n/a	Utah Slanted Array	n/a	n/a	Human, median nerve	Percept stability	72	E	Functionality decrease Delamination
Cui [39]	PI, Au, PI, PEDOT: PSS	MEA	EIS, CV	2	n/a	n/a	n/a	n/a	Cracking and delamination
Pranti [59]	PI, Au, PI, PEDOT: PSS	MEA	EIS, CV	<1	n/a	n/a	n/a	n/a	Delamination of coating
Nayagam [60]	Si, Pt, Si, n/a	MEA	Impedance	15	Cat, suprachoroidal	Histo, Impedance, AP	15	Lead failures	Tissue damage Threshold increase
Boehler [61]	PTFE, PtIr, PTFE, nanoPt	Wire	EIS, CV	5	Mice, frontal cortex	EIS, CV	5	E	Nano-crack formation
Čvančara [62]	PI, Pt-Ir-SiROF, PI, SiC	MEA	Impedance, optical	<1	Humans, rats	Impedance, Optical	4	E	Delamination
Pfau [13]	PI, Pt, PI, n/a	MEA	CV, mass loss	120 million pulses	n/a	n/a	n/a	n/a	Pt dissolution

Table 1: Summary of neural electrodes with chronic stimulation data. Sub: substrate material; Elec.: Electrode Materials; Ins.: Insulation material; Coat.: coating material; Si: silicon; Pt: platinum; Ir: iridium; Au: gold; w: width; t: thickness; D: diameter; EIS: electrical impedance spectroscopy; CV: cyclic voltammetry; SEM: scanning electron microscopy; E: experimental design; CH: conductive hydrogel; AP: action potentials; I: Insulation damage, MEA: Microelectrode array.

Protocols

The lack of a standardised protocol for characterising chronic stability is one hurdle faced in translating these devices from benchtop to clinical application. Recently, there has been research into developing a standardised framework for the characterisation of neural electrodes [63,64] and these protocols provide an extensive evaluation of the devices pre- and inter-implantation; however, there is still a lack of focus on post-implantation. Moreover, these protocols focus on collecting performance data *in vivo*, which is impractical for the rapid high throughput testing needed to

demonstrate chronic continuous functionality [40]. One alternative is to test the devices *in vitro* in a saline solution at temperatures of 37 ˚C and higher, known as accelerated ageing [65]. The Arrhenius reaction rate function can be used to determine the lifetime of the device at body temperature from the accelerated ageing mean time to failure. However, this method does not capture some of the degradation mechanisms that occur *in vivo*, such as the effects of proteins, thus resulting in dramatic differences in reported failure times [66]. The addition of oxidative species [43], and proteins [67] to the saline solution have been shown to replicate device degradation *in vivo* better; however, this is yet to be extensively investigated.

3. Neuromodulation

In neural tissue, the charge is carried by ions (sodium, potassium, and chloride) whereas within the electrode, the charge is in the form of electrons [20]. Therefore, there is a need for the transduction of the charge carriers from electronic to ionic, making the design of the electrode-tissue interface crucial to the success of neural implants [20]. Neural electrodes can be categorised into those which record neural activity and those which stimulate the tissue, with most research focused on the former. Stimulation electrodes aim to initiate a functional response from the neural tissue by eliciting depolarisation, in contrast to recording electrodes which aim to achieve a low signal-to-noise (SNR) ratio when detecting action potentials and low-frequency activities [68]. Recording electrodes operate at smaller potential differences and thus are much less at risk of inducing any adverse reactions; stable (> 5 years *in vivo*) recording electrodes have been achieved [69].

Stimulation electrodes face more complex challenges than passive recording devices due to the necessity of eliciting a response without causing any tissue damage. There is an empirical relationship between the likelihood of tissue damage resulting from electrical stimulation, the charge density, and the charge density per phase, as described by the Shannon criteria [70]. This is an increasingly important issue as electrodes become smaller and thinner, which leads to a reduction in the safe charge density limit due to the minimised electrode contact area [20,70,71]. As

a result, active stimulation electrodes have yet to demonstrate chronic stability (< 10 months *in vivo*) [68]. For these reasons, assuming that electrodes that are stable under active stimulation will be stable under passive recording, this review focuses on electrodes for neural stimulation. For an excellent summary of electrode devices for neural recording, the reader is directed to [72].

Stimulation Electrodes

For neural stimulation, electrical signals are injected into the neural tissue to elicit a response; stimulation induces depolarisation by driving the cell membrane potential towards its activation threshold [1]. This is achieved through the flow of ionic current between a working electrode and a counter electrode [68]. In this review, as consistent with publication nomenclature, the electrodes referenced are those designated as the working electrode.

The critical metrics of stimulation electrodes are safety and efficacy. An electrode is deemed safe if, during stimulation, there are no toxic by-products resulting from reactions at the electrode surface or compositional changes. All materials should be biocompatible, non-toxic, and irreversible faradic reactions should only occur at levels non-toxic to the tissue [1,68]. To ensure the efficacy of the electrode, the device should maintain good mechanical and electrical contact with the tissue. Mechanically, this requires electrodes of a similar stiffness to the target tissue (elastic modulus of ~100 kPa for brain tissue) to reduce glial scarring, while maintaining mechanical integrity upon application and micro-motion during the device lifetime. Electrically, the electrodes need to maintain sufficient charge injection to elicit the desired response while ensuring that the material's conducting, and insulating properties remain constant. A stimulation electrode's clinical usefulness depends on its capacity to deliver safe levels of therapeutic stimulation chronically. Maximising the clinical usefulness while addressing the above requirements presents one of the most difficult neural engineering challenges [28,73].

Charge-balanced biphasic waveforms are commonly used for stimulation as they prevent electrochemical reactions occurring at the electrode surface, thus reducing the chance of electrode

failure [68,74,75]. Unbalanced charges can lead to irreversible chemical reactions occurring at the electrode-tissue interface [20]; such reactions are undesirable as they can lead to pH changes, gas formation, and electrode dissolution due to the oxidative formation of soluble metal complexes [76,77]. However, even under continuous charge-balanced stimulation, an electrode may become polarised, due to erratic electrode potential changes, leading to irreversible faradaic reactions. Therefore, before implantation, the maximum charge density that allows charge injection by reversible processes must be experimentally determined and depends heavily on the electrode material. Small-area thin-film electrodes require materials with a higher charge injection capacity (CIC) as the charge injection density is proportional to the surface area of the electrode-brain tissue interface [18]. Developing electrode materials with a high CIC, thereby increasing the likelihood of eliciting an action potential before toxic irreversible reactions occur, is an emerging and vital research field [59,76,78,79].

4. Design of Thin-Film Electrodes

Thin-film electrodes typically comprise of three layers: the substrate, the metallisation, and the insulation or encapsulation layer (Figure 4). For this review, the effect of the interconnects and active devices such as amplifiers will not be considered. Within the layers, there are insulated tracks that connect the electrode pads to the external connections, and exposed electrode sites that are in contact with the tissue. Currently, devices translated into clinical application use 5-25 μm thick metal embedded into a 40-500 μm thick encapsulation layer which defines and insulates the electrode contact sites. The thicker the device, the higher likelihood of tissue damage upon implantation; this is the first driving factor behind the development of thin-film electrodes [18]. Secondly, to match the growing demand for high spatial resolution, there is a need for smaller electrodes that can be fabricated into higher density arrays. Thirdly, thin-films enable increased conformity, thus allowing for enhanced contact with the target tissue.

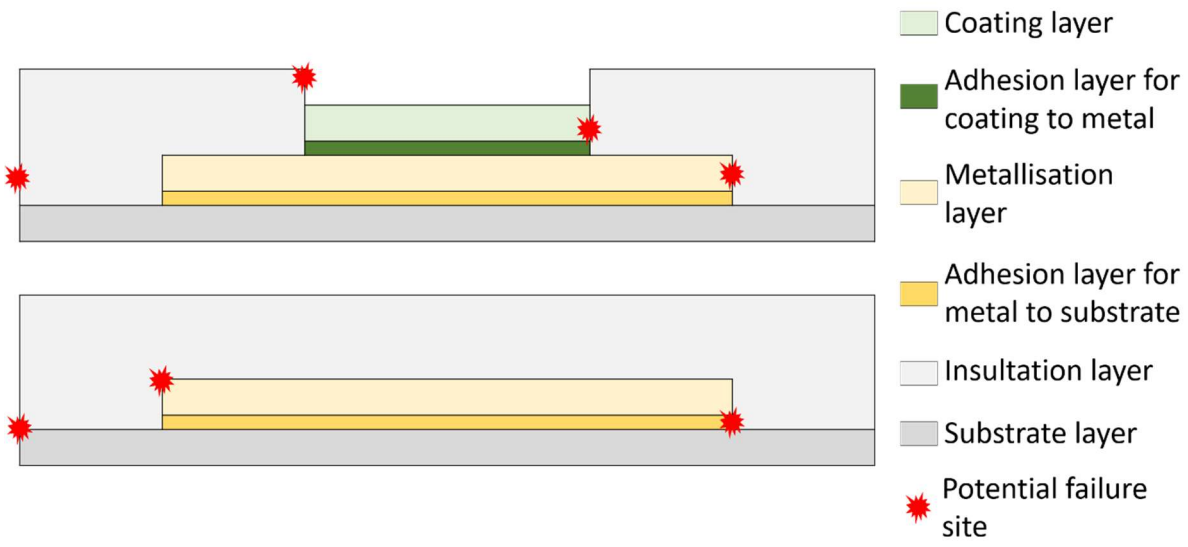

Figure 4: Example schematic of a thin-film electrode. Open electrode pads (top) and insulated electrode tracks (bottom). Stars mark weak areas of the electrode, namely the adhesion between the layers and areas open to attack from the aqueous environment.

4.1. Fabrication Methods

The manufacturing process of the chosen electrode material must be reproducible, scalable, and have a high resolution. Techniques such as standard photolithography, and chemical and physical vapour deposition are ideal for thin-film electrode fabrication [80], enabling nano and microscale scale features with high reproducibility and throughput for mass manufacture [17]. The standard protocol for electrode fabrication involves the deposition of a substrate layer coated with a thin-film of gold (Au) or platinum (Pt) using physical vapour deposition, from which electrodes are patterned photolithographically. Titanium (Ti) is usually deposited before the Pt or Au layer to improve adhesion. A thin layer of insulation material is then deposited on top of the metallisation and patterned such that the electrode contacts are open, and the interconnects are encapsulated. Additional layers are often deposited onto the open electrodes to reduce the electrode impedance and increase the charge injection capacity. For full details on fabrication techniques and example devices, the reader is directed to [17,81,82].

4.2. Substrate and Insulation/Encapsulation

As a base for the device, the substrate material must be biocompatible, biostable, chemically inert, possess good dielectric properties, offer mechanical integrity, and adhere to the metal electrodes. Once the metal electrodes have been deposited onto the substrate, insulation layers are necessary to prevent undesired current from spreading to neighbouring electrodes and non-target brain regions. An effective insulation barrier will prevent water from diffusing into the electrodes and forming a layer of moisture on the electrode tracks that can cause corrosion, dissolution, and leakage currents to flow between different electrode tracks [12]. The substrate and insulation layers are often made from the same material to provide a uniform interface and improve adhesion. The creation of an insulator-metal-insulator 'sandwich' allows for flexible electrodes with a reduced mechanical mismatch compared to that of pure metal electrodes [83]. Placing the metal electrodes in the middle of the 'sandwich' means they lie in the neutral bending plane, thus preventing the metal electrodes' cracking due to excessive strain (compressive and tensile). Lee et al. found that parylene-metal-parylene sandwiches had a minimum bending diameter of ~130 µm before fracturing, which could be further increased to ~450 µm upon deposition of an aluminium oxide (Al_2O_3) layer [84].

The ideal insulation material should possess properties including biocompatibility, favourable mechanical characteristics which address the compromise between stiffness for integrity on insertion and flexibility for conformity to the target tissue, good dielectric metrics including a low defect density to minimise the permeation of small molecules such as water and ions, and chronic adhesion to the metallic interconnects over large cyclic strains [85]. Through fatigue testing, Lee et al. found that 100% of parylene-metal-parylene electrodes failed after 100,000 bends [84]. The choice of encapsulation material is often neglected; however, the encapsulation material's surface area is large compared to the exposed metal electrode sites and thus often fails before the metallisation layer. A long term study *in vivo* (mean of 367 days) by Barrese et al. indicated that failure of the insulation material is the most significant factor in the reduction of both signal quality

and impedance of implanted electrodes [86]. The development of thin, defect-free layers of materials that can encapsulate such systems as robust biofluid barriers and, at the same time, as electrical interfaces to the surrounding biology represents a fundamental challenge, where operational timeframes may extend to the life of the patient (several decades or more). Table 2 summarises the key properties of different encapsulation materials.

4.2.1 Inorganic Layers

Inorganic materials are grown directly on top of the metallic layer by techniques such as atomic layer deposition (ALD) and chemical vapour deposition (CVD).

Silicon-Based

Silicon (Si) has previously been widely used in neural interfaces as a substrate layer and is currently one of the only insulating materials with full medical device approval [87]. The Utah and Michigan arrays are prominent examples of silicon-based electrode arrays but, despite their popularity, a long-term study by George et al. found that only 15 out of 113 and 0 out of 96 stimulating electrodes were functional prior to explantation [51]. Si devices commonly fail due to extrinsic defects such as pinholes resulting from the deposition processes. Moreover, the large mechanical mismatch between the rigid Si and soft neural tissue results in an increased foreign body reaction upon implantation, which reduces stimulation efficiency and leads to tissue damage [32]. Building on the well-established Si industry, silicon dioxide (SiO_2) has shown promise as a barrier layer, a few hundreds of nanometres, for thin-film electrodes. While films produced by chemical vapour deposition have high defect densities, thermally grown (oxidation temperature above 1100 ˚C) thin layers of SiO_2 are free from intrinsic and extrinsic defects offering effective isolation of the electrodes from the aqueous environment [88]. Fang et al. successfully integrated 1 µm thick films of thermally grown SiO_2 with flexible electronic structures using peel off from a Si substrate [88]. Their results implied that the limiting factor in the device lifetime was not the water permeation but hydrolysis rates of ∼80 nm/day at 90 °C. Extrapolation of hydrolysis rates predicted the lifetime of

these devices in the body to be a few decades. However, due to the capacitive coupling nature of thermally grown SiO_2, to avoid signal attenuation, either the thickness of the layers must be reduced (reducing the lifetime) or the lateral dimension must be increased (reducing the spatial resolution). Thus, large sensing pads are favoured which is not always realistic in microelectrode array fabrication [89]. To bypass this issue, one method uses patterned p-type Si nanomembranes bonded to the thermally grown SiO_2 to form a conductive pathway thus enabling electrical coupling and eliminating the capacitive layer [90]. These electrodes demonstrated a lower dissolution rate of 0.5nm/day at 37 °C and high conductivity with a sheet resistance of 32 Ω/sq. [90].

However, the dissolution of both Si and SiO_2 in aqueous environments limits their use for chronic applications [91]. While coatings can be applied to minimize such reactions, the introduction of additional materials and interactions is undesirable due to the necessity of further optimization.

Ceramic based

Aluminium oxide (Al_2O_3) is a ceramic often used as a protective coating for artificial joints and has proven long-term biocompatibility. Thin films of Al_2O_3 created by ALD technology, typically at 120 ˚C, have recently gained attention as a way to overcome the restrictions of bulk alumina. Moreover, ALD alumina has a water vapour transmission rate (WVTR) of 10^{-10} g mm m^{-2} d^{-1} [92], while polymeric materials have WVTRs in the range of 18 – 128 g mm m^{-2} d^{-1} [93]. However, in the presence of water, Al_2O_3 has been shown to undergo severe hydrolysis, thus multilayers of ALD Al_2O_3 and organic polymers are often utilized. Minnikanti et al. reported that the lifetime of an ALD (52 nm)–Parylene (6 µm) bilayer over 215 days in 60 ˚C saline, was five times greater than that of a Parylene-only coating.

Inorganic materials present a challenge in the form of heterogeneities in the growth process and contaminants which can lead to material defects such as pinholes and grain boundaries. To address the fact that these defects limit the lifetime of inorganic materials, research has been conducted on

multilayer encapsulation. Hogg et al. found that a multilayer of Parylene C (4.5 µm) and silicon oxide (3 x 4.7 µm) significantly reduces the permeation of water into the device [94].

4.3.2 Organic layers

Parylene and Polyimide

Conformable polymer-based layers have been proposed as an encapsulation material as they reduce the mechanical mismatch with the neural tissue, their electrical and mechanical properties can be readily tailored, and they satisfy high biocompatibility standards [33]. Polymers that have been utilised as substrates and encapsulation layers include Parylene C (PaC) and Polyimide (PI) [33]. PI has been used as a substrate layer in microelectronics due to its good dielectric properties and low permeability to water moisture with water uptake as low as 0.5 % [95]. PI is compatible with microfabrication and can easily be deposited via spin coating. However, it is not currently certified according to ISO 10993. Test samples sandwiched between 10 µm-thick polyimide layers soaked in saline at 75 °C saline failed after 66 day, equivalent to a lifetime of 2.5 years at 37 °C [96]. The PI samples underwent severe degradation upon soaking including dissolution, delamination, blistering, and corrosion [96].

PaC is a highly flexible polymer that can be easily deposited in thin layers *via* chemical vapour deposition to form pinhole-free barriers, offering chemical inertia and minimal permeability to water [97]. Unlike PI, PaC has acquired ISO 10993, USP Class VI rating. Using chemical vapour deposition allows for thin layers (< 100 µm), which reduces implantation damage and adds minimal weight [98]. However, such layers do not provide mechanical strength and are therefore often used in combination with silicone or alumina. Test samples encapsulated by 10 µm thick PaC layers soaked in 75 °C phosphate-buffered saline (PBS) failed after 117 days as a result of blistering and delamination [96]; the expected lifetime of this sample device at 37 °C is about 4.5 years. While polymer substrates can offer increased conformability and flexibility, their key characteristics of

WVTR, ion permeability, and adhesion capability to noble metals need to be optimised for specific applications [99].

Liquid-Crystal Polymers

Liquid-crystal polymers (LCPs) represent a promising field in encapsulation materials due to their low moisture absorption rate (Table 2), low free volumes, and efficient chain packing. Such electrodes are fabricated from thin-films of commercially available LCP sheets. To form the LCP/metal/LCP sandwich, a high melting temperature LCP substrate is patterned with the metallization layer and then thermally bonded to a layer of low melting point LCP [100]. Lamination of the LCP on the top and bottom sides of the electronics provides robust barrier function *in vivo*. Test samples of the basic LCP/metal/LCP sandwiched structure soaked in 75 °C saline failed after 379 days, due to water infiltration through the LCP-LCP bonding which resulted in complete delamination of the LCP layers [96]. Accelerated ageing results from these studies highlighted that the weakest interface was the LCP-metal adhesion around the electrode openings. One limitation is the low optical transmittance of LCPs which makes the alignment of layers difficult and reduces the application for cell culture and optical microscopy [100].

SU-8

SU-8 is a commonly used epoxy-based photoresist comprised of a photo-acid generator compound with an incorporated solvent. Due to its mechanical and chemical stability and ease of nano fabrication, it has been used as a high aspect ratio structuring material offering optical transparency, an advantage over silicon and LCPs. While SU-8 has not yet obtained the USP Class VI rating for biocompatibility, preliminary studies have shown its use as a substrate and encapsulation material for electrodes [101,102]. However, further biocompatibility and long-term studies are needed to validate its use.

PEN and PET

Polyethylene napthalate (PEN) and terephthalate (PET) are common materials used in the food packaging industry due to their excellent abrasion resistance, electrical insulation, and

biocompatibility. PEN offers high light transmittance compared to PI and PaC (Table 2), while also costing significantly less than PI. The main challenge with these materials is their low heat transition and glass transition temperatures (< 120 ˚C) which make them hard to manufacture with most electrode fabrication techniques. Recently, Kaltenbrunner et al. developed an ultra-light weight, low cost, 1 µm PEN based microarray by using temperature-independent fabrication processes [103]. Kunori et al. developed a transparent epidural electrode using indium tin oxide (0.1 µm) coated PET (0.127 mm). Indium tin oxide is a conducting polymer that does not require any thermal evaporation and thus can easily be deposited on PET films [104].

Silicone Elastomer

Polymers that contain silicon are known as silicones; they have a characteristic backbone of repeating silicon-oxygen bonds. Polydimethylsiloxane (PDMS) is the most commonly used silicone, where the silicon atoms are bonded to organic methyl groups. PDMS offers excellent, and proven, biocompatibility as well as high flexibility and mechanical stiffness close to that of neural tissue. PDMS has a much lower fabrication cost compared to PI, as demonstrated by Cabello et al., who used micro-milling to develop a low-cost gold MEA embedded in 2 mm PDMS [105]. Guo et al. developed a 60 µm thick PDMS-based integrated stretchable electrode array, however they highlighted the fact that PDMS is not a hermetic material and for chronic applications multilayers may be needed [106]. One study has shown that an additional 5 mm-thick coating silicone elastomer on top of a 40 µm-thick PaC layer could extend the expected lifetime of the test samples from 2.5 to 6.7 years at body temperature, based on accelerated ageing at 85 and 97 °C PBS, during which failure was defined as the resistance value falling below half of the initial value [107].

Material	Encapsulation (E), substrate (S) or both (B)	Deposition Method	Optical transmittance at 380 nm (%)	Water absorption (%)	Youngs Modulus (GPa)	Tensile strength (MPa)	Thickness (µm)	Predicted lifetime at 37 ˚C from accelerated ageing (Years)	Reference
Si [1]	S	Spin	-	N/A	140	165	25	1.06**	[86]
SiO_2 [2]	B	Thermal	91-88	N/A	74.8	155	0.1	70	[88]
Al_2O_3 [3]	B	ALD	61	N/A	344.83	154	0.052	2 days*	[108]
Polyimide [4]	B	Spin	80	2.0-3.0	2.5	128	10	2.52	[96]

Parylene C [5]	B	CVD	82	< 0.1	2.8	69	6	1.64	[108]
	B						10	4.46	[96]
	B						40	2.4	[107]
SU-8 [6]	B	Spin	75	0.55	2	60	1	30 days **	[109]
PEN [7]	S	Spin	90	0.4	2.7	55	1.2	4 weeks **	[110]
PDMS [8]	B	Spin	85	0.25	0.57	5.13 - 7.65	<100	5.5	[111]
LCP [9]	B	Thermal bonding	20	0.04	19	180 - 190	25	7.6	[112]
							50	10	[112]

*Table 2: Comparison of material properties for substrate and encapsulation layers. [1] University Wafers, Silicon,[2] Thermally grown on Silicon University Wafers,[3] Sigma Aldrich, Aluminum Oxide, [4] HD MicroSystems, PI-2525, [5] Specialty Coating Systems, Parylene C, [6] Microchem, SU-8 3000, [7] GoodFellow, PEN, [8] Dow Corning, Sylgard 184, [9] Kuraray, Vecstar. * increased to 6 years in bilayer with 6um PaC, ** Based on in vivo or in vitro testing not accelerated ageing.*

4.3. Metallisation

The metallisation layer enables signal transduction between the electrode's electrical charge and the ions flowing in the body tissue. Ideal metallisation layers will have a high CIC (Table 3) to elicit action potentials without causing any reversible reactions and will be resistant to corrosion under stimulation. Noble metals such as Pt, Au, and Iridium (Ir) are often used due to their high resistance to corrosion and excellent biocompatibility properties [34,42,113]. Thin-film Pt layers are industry standard as they can be easily micromachined to nano-metre scale features. Pt has demonstrated high biocompatibility and non-toxic use in epiretinal arrays [114] and cochlear implants [115]. However, for stimulation, there has been investigation into the cytotoxicity of Pt-based by-products of dissolution and corrosion [116–118]. Shepherd et al. found that chronic stimulation (6 months, charge density 267 µC/cm^2/phase) of Pt electrode arrays resulted in significant production of Pt particulates and an increase in fibrous tissue response [118]. While both Pt and Au corrode when used for stimulation purposes, Ir has demonstrated its capacity as a noncorrosive stimulating electrode [119]. The stable formation of activated iridium oxide (IrOx) on the electrode surface, enhances its corrosion resistance while offering a high CIC. Frederick et al. developed a potential pulsing high rate method for the fabrication of activated iridium oxide film electrodes with charge storage capacities (CSC) of 33.3 mC/cm^2 [120]. Another material considered for thin-film metallisation is titanium nitride (TiN), which has a high effective surface area due to its columnar structure which increases the electrode's CIC [121]. Rodrigues et al. presented an 80 x 80 µm

titanium nitride-PI microelectrode with a CIC of 1.54 mC/cm^2 [122]. An alternative to using metal tracks is the use of glassy carbon which does not undergo corrosion, as demonstrated by Vomero et al. [123].

Material	**CIC (mC/cm^2)**
Pt	0.83
Pt-PEDOT:PSS	2.71
Au	0.2
Au-PEDOT:PSS	1.90
IrOx	1-5
TiN	1

Table 3: Comparison of the CIC of different metallisation layers and coatings [68,124].

Electrode Coatings

While noble metals offer high conductivity and resistance to electrochemical breakdown during stimulation [125–130], they typically have a low CIC and CSC, which restricts the amount of charge they can deliver to cells [74]. The need for higher CIC limits has resulted in the proliferation of new coating materials that increase the electrode surface area and thereby increasing its CIC. One such example is conducting polymers (CP) which achieve larger CICs and CSCs, resulting in greater neural stimulation [131]. The CP poly (3,4-ethylene dioxythiophene): polystyrene sulfonate (PEDOT: PSS) has been shown to increase the CIC of a Pt electrode three-fold for microelectrodes of the same dimension [132]. Moreover, the reduced mechanical mismatch between the CP electrodes and surrounding tissue decreases fibrous tissue formation and, subsequently, the electrode-tissue impedance [71]. This further increases the CIC, enabling injection at lower voltages and reduced power consumption [131]. CPs also exhibit anti-corrosive properties and minimise the dissolution rate [131]. With the addition of any coating material, there needs to be consideration of the increase in cross-sectional area and additional by-products [133]. The manufacture of thin-film devices often

leaves a ~2 µm gap (the insulation layer's thickness) [82] between the sunken electrode and the neural tissue, resulting in fluid separating the electrode and neural tissue (Figure 4). The distance between the electrode and the target tissue is critical for determining the stimulation's amplitude. The deposition of a thin-film coating can reduce this dimension and maximise the contact between the electrode and neural tissue, thereby maximising the stimulation efficiency and SNR.

5. Failure Modes

In an aqueous environment, such as neural tissue, and under constant mechanical forces from acute brain movements, stimulation electrode failure can be rapid [134]. Processes that can limit an electrode's lifetime include: damage to the electrode's metallisation layer via corrosion or strain-induced cracking, delamination resulting from adhesion loss between layers [135], and failure of the insulation layer from pinholes or water permeation [136–138] (Figure 5).

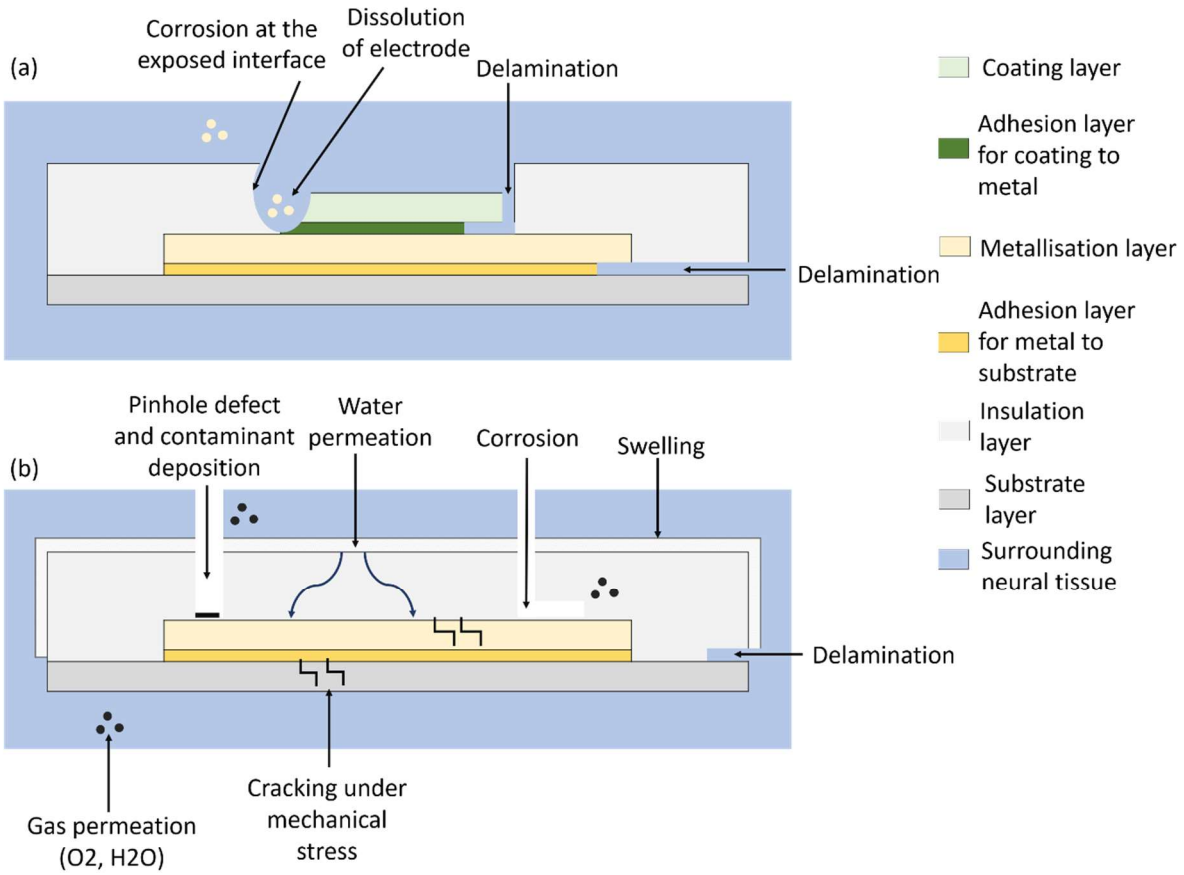

Figure 5: Schematic representative of the failure modes of (a) open metal electrodes and their adhesion layer, and (b) insulated metal tracks in an aqueous biological environment represented in blue.

It is paramount to identify the failure cause to prevent repeat failures and optimise the electrode's stimulation efficiency. This process is often neglected in the literature; on occasions where a failure is reported, no in-depth analysis is carried out on the failure mode [29]. To summarise the available clinical data on the failure of thin-film electrodes for neuromodulation, a systematic search of the MAUDE 2 database was performed looking between 01/01/2010 and 31/12/2020, inclusive [139]. The MAUDE database is a collection of voluntary reports detailing adverse events arising from faulty medical devices. An initial search was performed using the key terms "thin-film" AND "electrode" AND "neuro" which generated 19 results. To broaden the search scope, only the keywords "electrode" AND "neuro" were surveyed with a range of different failure modes. As highlighted in Table 2, electrode fracture is one of the most frequent failure mechanisms, followed by swelling of the device and delamination. While mechanical strain was not reported directly, mechanical failures are included in the "fracture" search as these may refer to the failure of the electrode along the device bending plane. However, this sample only represents those manufacturers who have reported device failures and, unsurprisingly, most reported failures included minimal information about the cause. The results in Table 4 are similar to those found in searches which considered a broader range of clinical applications [22,140].

Term Surveyed ("Electrode" AND "Neuro" AND)	**Number of Reports**	**Severity Ranking**	**Reported adverse effects**
"Failure"	229	N/A	N/A
"Fracture"	103	1	Increased fibroblast and macrophage activity [141].
"Delamination"	12	2	Intraparenchymal bleeding [142]
"Swelling"	2*	5	Pinching of nearby blood vessels
"Corrosion"	1	3	Induced cell death, loss of metabolic activity [116].
"Dissolution"	0	4	Increased fibrous tissue and macrophage response [118]. Mitochondrial swelling [116]

Table 4: Summary of the survey of electrode device failures performed using the MAUDE database. The total number of reports does not sum to 229 due to other unsurveyed failure mechanisms including surgery, battery and lead failures . 33 results for swelling, however, 31 of them were reports on tissue swelling. Severity ranking based on the number of reported adverse patient effects and failure frequency.*

5.1. Fracture and Cracking

Neural electrodes are under continual cyclic loads and strain due to acute brain movement over the implant's lifetime, which often leads to the bending and cracking of the metallisation layer [84]. The bending strain exerted on the thin-film electrodes is a function of the distance between the metal film and the neutral plane. Thus, the metal layer should be positioned at the device's neutral bending plane to minimise the electrode's strain [143–145]. While this is possible for the insulated tracks, the open electrode contacts will not be in the neutral plane. To minimise the bending strain, and the chance of mechanical failure by cracking, the substrate layer should be fabricated as thin as possible while retaining the mechanical stability [146]. Lee et al. found that metal traces in the middle of 24 μm thick Parylene–metal–Parylene devices had a minimum bending diameter of ~130 μm before breaking [84].

5.2. Adhesion and Delamination

Delamination is reported as one of the most frequent failure mechanisms of thin-film electrodes, whereby two layers (insulation-metallisation or metallisation-electrode coating) separate from one another [49,135,147]. Delamination can occur because of water intrusion at the interface, which leads to a change in adhesion due to the weakening of polar attractions and/or mechanical interlocking. It can also occur due to cyclic mechanical stress which fatigues and eventually breaks the poor adhesion [135]. Delamination between the metal and insulation layers can cause current leakage into undesired areas of neural tissue, an increase in current density leading to electrode dissolution, corrosion of metallic interconnects, and cracking of metallic layers.

Polymers commonly used for insulation materials exhibit poor adhesion to the inorganic metallisation tracks because the polymer and metal atoms are unable to form compounds [10]. Polymer-based insulation materials are selected for their chemical inertness; however, this results in reduced adhesion to the metallisation layer. The adhesion instability between polymer and metal electrode is exacerbated by the aqueous conditions present in neural tissue. All polymers exhibit

some permeability to gases, including water vapour, however by altering their crystallinity and composition this can be minimised, thereby improving their functionality as a barrier layer [148]. Polymer chains expand and plasticise upon water absorption, thereby enabling further diffusion of water, salts, and ions into the interface. This expansion can induce stress in the neighbouring layers leading to cracking (if adhesion strength exceeds cohesion strength) or delamination (if cohesion strength is greater). In addition to its mechanical effects, water incursion also affects the bonding between the layers by altering the polymer's polarity, increasing water permeability [149].

Prasad et al. conducted a comprehensive study into the biotic and abiotic failure modes of Pt/Ir electrode arrays six months after implantation. It was found that 21% of electrodes failed due to either delamination or cracking of the insulation [47]. Čvančara et al. found that 62.5% of explantation stimulation electrodes experienced delamination of the thin-film metallisation from the PI-Pt interface after 30 days *in vivo* [62]. This was one of the earliest clinical human studies to report failure mode results from the explantation of stimulation electrodes [62]. Through systemic failure mode analysis, the adhesion between the PI-Pt layers was identified as a weak point and was subsequently optimised through the addition of silicon carbide. This study highlights the efficacy of failure mode analysis to guide implant stability optimisation. While 30 days is not a sufficient period on which to base chronic measurements, Čvančara et al. published some of the first analysis of how and why their electrodes failed, and this should act as a framework for other studies.

Analysis of delamination failures is further complicated because the stimulation electric field's strength strongly impacts PaC's lifetime. Li et al. found that active devices under accelerated saline testing failed within two days due to PaC delamination, while passive devices of the same thickness took up to 70 days to fail [150]. Further testing and modification of the polymer layer is needed to ensure stability under chronic continuous stimulation.

5.3. Swelling

As mentioned above, the swelling of polymer layers due to increased plasticity upon water uptake can lead to either delamination or cracking of the metallisation layer. Polyimide, for example, swells by approximately 4-6% (w/w) upon implantation [151]. Aside from its adverse effects on adhesion, swelling can also reduce contact between the electrode and target tissue, dramatically inhibiting the device's effectiveness. For stimulating electrodes, a quadratic relationship exists between the threshold current required for extracellular stimulation of the neurons and the distance between the electrode and target tissue [152]. Thus, an increase in the insulation or coating volume will increase the required threshold current, thereby increasing the necessary electrode current density and the ultimate likelihood of failure. Depending on the electrode's design, swelling of the polymer contact coating may either increase or decrease the distance between electrode and tissue [153–155]. If the electrode is sunken into the insulation layer, then swelling of the electrode coating will bring the electrode closer to the tissue; if the electrode is raised above the insulation, the opposite occurs. Thus, swelling must be considered during electrode design and is further complicated by the dependence of swelling on the electric field strength [153].

5.4. Corrosion

Electrode corrosion has been a long-standing concern regarding chronic neural implants, as such the effects of corrosion on available biomaterials have been reviewed previously [119]. Corrosion processes are exacerbated in the aqueous conditions of neural tissue due to complexing agents such as chloride [117,118] and increased concentrations of reactive oxygen species, such as inflammation-induced hydrogen peroxide [25,32]. During stimulation, corrosion is also accelerated by charge imbalanced-induced irreversible reactions at the electrode surface [20,156].

Thin-film electrodes dimensions are within a few tenths or less of a micrometre [157]. At these dimensions, the electrode size is similar to that of the diffusion layer at the electrode-electrolyte interface. This means that the electrodes undergo spherical diffusion instead of linear diffusion like

macroelectrodes [21]. As a result, there is increased mass transport and higher reaction rates for the faradaic charge transfer between the electrode and dissolved species in the aqueous surroundings. The increased rate of chemical reactions occurring at the electrode surface increases the likelihood of corrosion [119].

The most corrosive components within neural tissue are dissolved salts, namely chloride ions. In solutions without complexing substances, Au and Pt are immune to corrosion throughout the entire water stability domain (Figure 6). However, the introduction of chloride ions into the system results in regions of corrosion-prone soluble Pt/Au-chloride complexes. Preventative measures are needed to forestall these complexes from forming and accelerating the corrosion rate. Previously, electropolishing of the electrode surface has been employed; however, this counteracts the additional CIC advantages of a rough surface [158]. Alternatively, a coating material such as a conductive polymer can be deposited on top of the metallisation to improve the electrode's resistance to corrosion [119]. Corrosion is also worsened by reactive oxygen species (ROS) production, namely hydrogen peroxide, by activated microglia as part of the foreign body response to the implant [159]. ROS have been shown to persist for up to 16 weeks, and such long-term

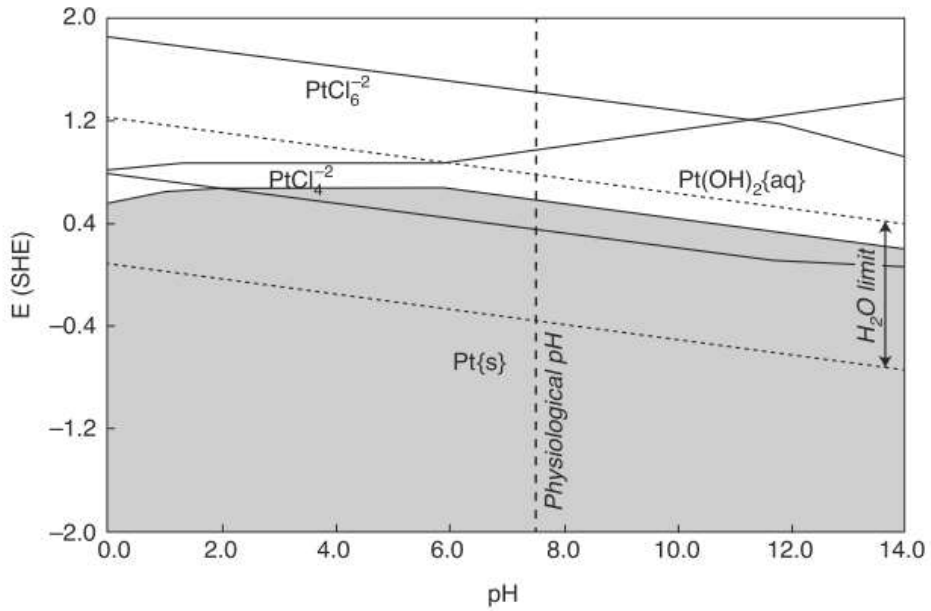

Figure 6: Pourbaix diagram outlining the stability of Pt in PBS with 30 mM H_2O_2, illustrating the corrosion resistance as a function of pH value and electrode potential. The addition of Cl ions shifts the stability away from equilibrium. Reproduced from [64].

exposure can lead to electrode degradation [160]. Corrosion results from the oxidation of the metal electrode to the lowest available stable valence state. As the concentration of oxygen (in the form of ROS) surrounding the implant increases, so too does the rate of corrosion [119]. Production of ROS can also affect the pH around the implant, as the pH is shifted away from equilibrium it will affect the corrosion rate constant, leading to an increase in corrosion. Resistance to corrosion due to oxygen species can be improved by incorporating a passivation layer such as a metal-oxide thin-film.

Failure due to corrosion is more common in stimulation electrodes than recording electrodes because of the active injection of charge. Corrosion due to charge imbalance can effectively be mitigated with charge-balanced biphasic waveforms that prevent electrochemical charge build-up at the electrode-tissue interface [74]. However, there are some circumstances where, even with charge-balanced pulses, the electrode becomes polarised. For example, Morton et al. found that corrosion occurs on a gold electrode in phosphate-buffered saline with charge-balanced neural stimulating conditions [161]. Experimental optimisation is needed to define the stimulation limit for new electrode materials.

5.5. Dissolution

Dissolution of the metallisation layers results from electrode corrosion during stimulation, which leads to the breakdown of the electrode [77,162–165] and the production of toxic by-products [166–168]. It has been found that the dissolution of Pt in saline increases linearly with injected charge during biphasic pulse stimulation [77]. Dissolution was also reported by Pfau et al. when measuring the dissolution rate of Pt using inductively coupled mass spectroscopy [13]. This study investigated dissolution rates in a saline solution *in vitro*; however, the results *in vivo* are likely to differ due to proteins in the neural tissue. Proteins can exacerbate corrosion and dissolution by binding to the metal ions and removing them from the electrode surface and destabilising the electric double layer. However, proteins can also inhibit corrosion by adsorbing onto the electrode surface and acting as a

barrier between the metal and the surrounding tissue [164]. The complicated and opposing nature of these interactions requires further investigation.

6. Failure Mode Detection

To achieve the next technological breakthrough in neural implants, there needs to be an increased understanding of electrode interactions with the surrounding tissue and subsequent systematic analysis of their failure modes. This calls for the implementation of more comprehensive reporting and analysis systems to capture the failure mode and enable electrode optimisation to produce chronically stable and clinically translatable electrodes. Different techniques include those that are optically, mechanically, and electrically based (Figure 7).

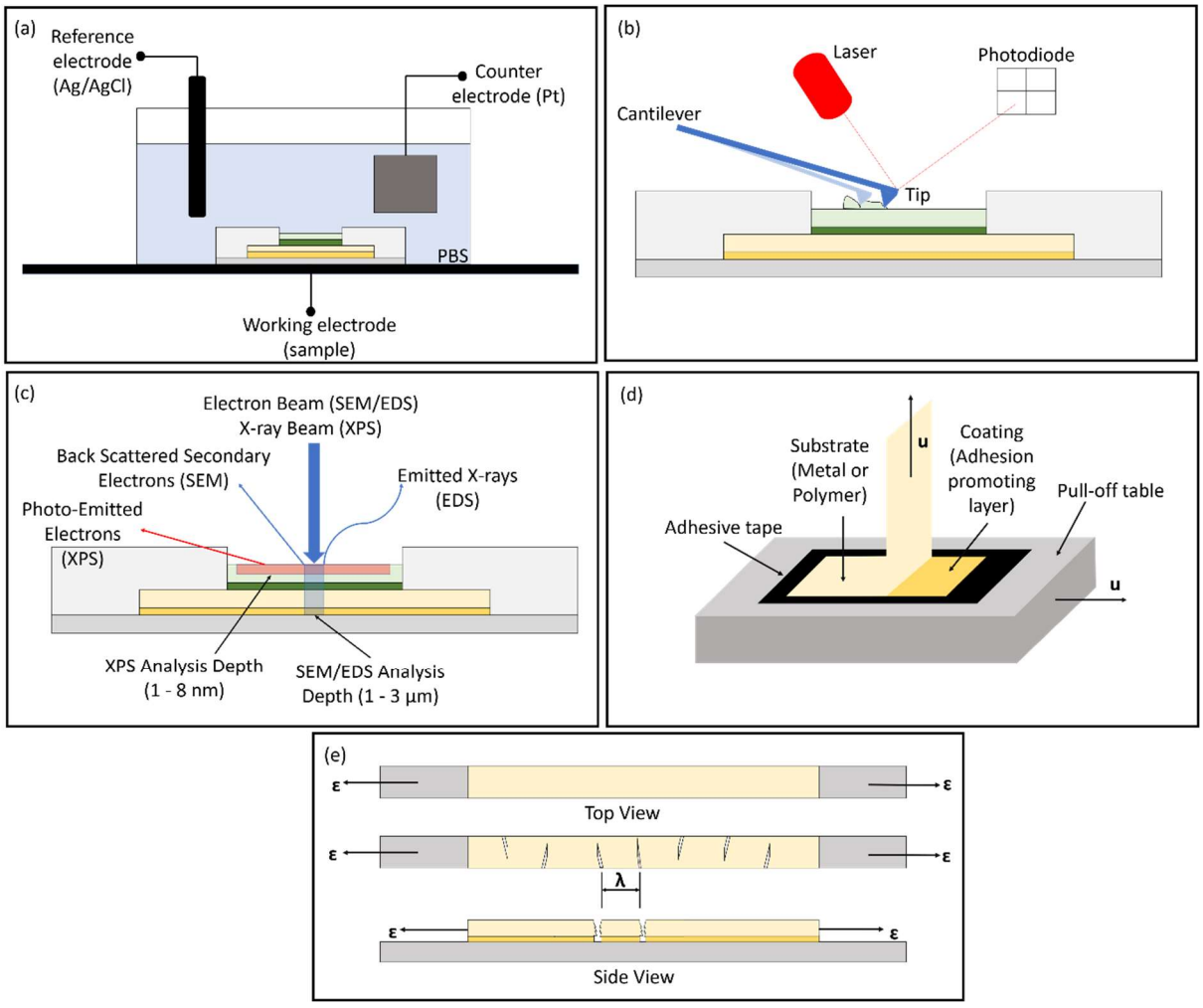

Figure 7: Failure mode analysis techniques. (a) EIS set-up for electrical characterisation. (b) AFM interactions to measure surface topography. (c) Interaction of SEM, XPS and EDS with the electrode sample. (d) Peel 90˚ test to measure the adhesion between different layers where u is the applied force. (e) Tensile test to measure the adhesion between layers, where ε is the applied strain and λ is the distance between cracks.

6.1. Electrochemical Impedance Spectroscopy (EIS)

Continuous impedance measurements give great insight into the real-time electrical performance and viability of implanted electrodes [45,47,169] (Figure 7a). By measuring the impedance and phase shift of the current through the electrode as a sinusoidal potential is applied, the electrode's electrochemistry in a given medium can be analysed [170]. The electrochemical impedance is obtained by comparing the amplitude and phase of the applied signal with the recorded output signal over a range of frequencies. Impedance measurements provide a diagnostic measure to identify the electrode failure mode, making EIS one of the most common tests to determine electrode performance [47,171–176]. High impedance values are indicative of electrode damage and contact corrosion. Barrese et al. observed a ten-fold increase in implantable cortical electrodes' impedance magnitude, which alongside explant SEM analysis confirmed cracking of the Pt electrode [49]. Low impedance values are symptomatic of insulation failures, as reported by Kozai et al., who observed a drop in impedance coinciding with the breakdown of the silicon oxide insulation [177]. The insulation's long-term performance is critical in determining the device stability as it has significant implications for its efficiency. Impedance values can also be used to identify fluid ingress under the insulation layers. Fluid ingress provides conductive pathways between adjacent electrodes and can significantly reduce stimulation efficacy. By comparing the impedance of adjacent electrodes to that of isolated electrodes, the magnitude of fluid ingress can be determined [87].

More recently, impedance analysis has been used to determine biotic failure mechanisms in addition to abiotic. Cody et al. reported that real-time impedance data was reflective of the mode of foreign body encapsulation of the electrode. Fully encapsulated electrodes displayed a sharper decrease in impedance over six weeks when compared to partially encapsulated electrodes [176].

6.2. Surface Topography of Electrodes

While EIS can diagnose electrical failures within the device, further analytical measures are needed to complement and validate the data. Surface analysis of the electrode arrays before and after

stimulation provides information about the electrode surface's quality and longevity. Surface features that can be identified include mechanical degradation, metal dissolution, surface contamination, and corrosion. In addition, looking at cross-sectional surfaces reveals the extent of delamination. While optical microscopy can be used to analyse features with a 200-500 nm resolution, the limiting resolution of the wavelength of light means surface level failures may be missed [178]. Super-resolution microscopy techniques that are not limited by diffraction can be used to visualise sub 100 nm scale features.

6.2.1. Atomic Force Microscopy (AFM)

AFM is a common technique used to measure surface topography and identify surface abnormalities in insulation adhesion or cracks in the material [179] (Figure 7b). The surface's average roughness and height can be determined by measuring the deflection of a cantilevered probe across the surface. While no defects were identified with optical microscopy, through AFM, Geninatti et al. found that the roughness of sputter-deposited platinum electrodes increased in response to an applied potential [173]. This was attributed to an increase in metal dissolution at potentials higher than the water window. In contact-mode, AFM measures the pull-off force between two surfaces, from which the adhesion force can be determined to investigate the stability of a variety of adhesion promoters [180].

6.2.2. Scanning Electron Microscopy (SEM)

To further analyse the failure mechanisms of thin-film electrodes, scanning electron microscopy (SEM) can be used to visualise structural changes on the electrode surface including delamination and cracking [45,49,58,79,181], with a resolution of 5-10 nm (Figure 7c). Using SEM, Barrese et al. identified progressive corrosion of Pt microelectrode arrays and delamination of the PaC insulation, which led to the failure of 6 out of 8 chronically implanted devices [49]. SEM may also be used in combination with focused ion beam spectroscopy to gather high-resolution cross-sections of the different layers [62].

6.3. Elemental Composition Analysis

Elemental composition analysis of the electrode surface and surrounding tissue provides quantitative data about electrode composition changes resulting from continual stimulation. Electrode dissolution, contamination, and delamination can all be identified using elemental composition analysis.

6.3.1. Energy Dispersive X-ray Spectroscopy (EDS)

SEM with energy-dispersive X-ray spectroscopy (EDS) provides a surface level overview of the structure of the electrodes and the elemental composition of a selected area by analysing X-ray radiation patterns caused by the electron beam interacting with the sample [181] (Figure 7c). Using EDS to examine the surrounding tissue of an explanted activated iridium oxide film, Cogan et al. found that over-stimulation led to the degradation of iridium oxide into the cortical tissue [182].

6.3.2. X-ray photoelectron spectroscopy (XPS)

A promising technique in identifying adhesion problems at electrode layer interfaces is X-ray photoelectron spectroscopy (XPS). XPS uses a beam of electrons to analyse the top 5-10 nm of a surface [179] (Figure 7c). XPS can be used to complement the EDS data and provide more surface sensitive and chemical bonding data; this is particularly important when analysing adhesion layers [40]. Scholten et al. used XPS to determine when their Pt films had fully delaminated from PaC substrates, observing that no Pt was detected on top of such films [99].

6.4. Adhesion Testing

With the development of novel biomaterials and coatings, tests are needed to evaluate their long-term adhesion stability. This is partially addressed by methods such as the crosscut test and peel test, which can be performed *in vitro* pre-implantation [135,147,183,184]. The former involves artificially cutting the electrodes and applying an adhesion force to evaluate the extent of

delamination. Doing so mimics the effects of electrode delamination due to pinhole defects in the insulating layer. Peel tests involve immersing the electrode into a saline solution with one end attached to a load cell and another to a fixed point; a force is then applied until the layers peel away from each other (Figure 7d). This is considered a more representative test method as it does not rely on an artificial cut in the electrodes, which is harder to control and a less common scenario in electrode failure [99]. However, these approaches have limitations with regards to thin films on metallic surfaces [185]. To resolve these limitations, Martin et al. proposed a tensile testing method that involves analysing the periodic cracking of the thin-film (Figure 7e) [186].

7. Improving Stability

Depending on the failure mode, there are several methods for improving adhesion (Table 5). Due to the frequency at which delamination occurs, numerous studies on improving the intra-layer adhesion have emerged. The initial focus was on improving the adhesion between the metallisation tracks and the polymer substrate or insulation layer. Oxygen plasma has been successfully applied to roughen the surface of different layers, which aids interlocking between the thin-films [56]. While mechanical interlocking provides some adhesive strength, oxygen plasma treatment also modifies the chemical adhesion between the layers, which has a higher adhesion strength. For improved chemical adhesion, oxygen treatment can increase the number of carbonyl groups at the metallisation surface, leading to increased binding sites for the polymer insulation layer [187,188]. On their own, organic polymers are unable to form stable carbides with the inorganic metal electrodes; this can be mitigated by depositing titanium or chromium metallisation as adhesion-promoting layers for Au or Pt contacts. These transition metals can form long-term stable carbides with the noble metal electrodes and the polymer layer, thereby increasing stability [189]. The formation of carbon-metal bonds is another rarer type of adhesion mechanism between polymers and metals. Unlike oxygen treatment, this adhesion should take place in oxygen-free conditions. While this method has had some success in improving stability, introducing a secondary metal

increases the likelihood of corrosion and the likelihood of device failure due to the difference in the two metals' half-cell potentials.

Adhesion Promoter	Deposition Method	Thickness (nm)	Plasma	Gold Deposition Method	Gold Thickness (nm)	PaC Deposition Method	PaC Thickness (um)	Adhesion Force (mN/mm)	Reference
Ti	E-beam evaporation	30	CF_4	E-beam evaporation	300	Gorham	5	1.29	[190]
Ti	Sputter	30	Ar	Sputter	300	Gorham	10	35.5	[191]
DLC	PE-CVD	100	Ar	Sputter	300	Gorham	10	6.3	[191]
Ti + SiO_x	Sputter, PE-CVD	100	Ar	Sputter	300	Gorham	10	5.1	[191]
TMS	PE-CVD	105	Ar	Sputter	300	Gorham	10	Delaminated	[191]
Silane A174	Immersion	100	Ar, O_2	Sputter	300	Gorham	10	157.5	[191]
Cr	E-beam evaporation	20	-	E-beam evaporation	200	Gorham	10	3	[192]
Cr	E-beam evaporation	20	O_2	E-beam evaporation	200	Gorham	10	3.5	[192]
Cr + Silane A174	E-beam evaporation, Immersion (30 min)	20	-	E-beam evaporation	200	Gorham	10	110	[192]
Cr + Silane A174	E-beam evaporation, Immersion (30 min)	20	O_2	E-beam evaporation	200	Gorham	10	100	[192]
Ti + TMS	E-beam evaporation, PE-CVD	20	Ar	E-beam evaporation	200	Gorham	1.5	230	[193]
Ti + TMS	E-beam evaporation, PE-CVD	20	O_2	E-beam evaporation	200	Gorham	1.5	320	[193]

Table 5: Adhesion force stability obtained from the peel 90˚ test for Parylene C-Au interfaces for a range of different adhesion promoters. Where: titanium (Ti), carbon tetrafluoride gas (CF_4), silicon oxide (SiO_x), diamond-like carbon (DLC), tetramethylsilane (TMS), oxygen gas (O_2), Argon gas (Ar), chromium (Cr) and plasma-enhanced chemical vapour deposition (PE-CVD).

Inorganic interlayers have been investigated as a possible way to mitigate the effects of bi-metallic devices. One such example is incorporating silicon carbide (SiC) [62] to improve the adhesion between PI and Pt. SiC enables the formation of an additional carbon-carbon bond with the PI and forms stable carbide bonds with the Pt. Initial studies with SiC have indicated stability *in vitro* for up to 7 weeks and should be considered for future investigation [62].

As research interest in electrode coatings has increased, there has been parallel research into improving the adhesion between coatings and metallic electrodes. Several methods have been reported to enhance this adhesion in aqueous environments such as neural tissue. These include topographical modification of substrates by increasing the roughness of the metallisation [59,194] and electrodeposition of chemically modified 3,4-Ethylenedioxythiophene (EDOT) monomers that increase the number of functional groups [195]. While these methods have shown some success, they require modification of the EDOT monomer and can only be achieved through

electrodeposition, limiting their use in thin-film electrodes. Inoue et al. have been developing a hydrophilic polymer adhesive that can form a strong adhesion to a range of substrates, such as Au, while forming an interpenetrating network within the conductive polymer [183]. This adhesive can be deposited by solvent casting and spin-coating, which are more advantageous for the fabrication of thin-film electrodes. These methods show promise in addressing the adhesion challenges, but further studies are needed *in vivo* to evaluate their long-term stability performance under chronic continuous stimulation.

8. Summary and Conclusions

While research into neural implants is experiencing exponential growth there is a dearth of studies into thin-film electrodes' stability for chronic neurostimulation. New materials for the substrate, metallisation, and encapsulations layers need to be explored and carefully selected to reduce the likelihood of failure and increase stimulation efficiency.

Thin-film electrodes with a high spatial resolution and sensitivity have demonstrated their potential as recording electrodes, but their application as stimulation electrodes requires further investigation. This review highlights the need for a change in the approach to investigating and publishing electrode failure. The lack of published failures and subsequent analysis has limited the optimisation of such devices, and the scarcity of long-term clinical studies raises concerns about their safety. While some groups are beginning to publish investigations on explanted electrodes, there still needs to be a field-wide acknowledgement that studying device failure and degradation will enable the fabrication of better devices. It must be acknowledged that the optimal device, which many groups are striving for, will only come to fruition if there is in-depth investigating into preventing device failure.

Long-term stability under continuous stimulation will not be possible until the issues of delamination, corrosion, and swelling are addressed. One promising area of research includes the development of new contact coatings to improve stimulation efficiency. While these materials offer

a high CIC, their adhesion to metal electrode contacts is poor in aqueous conditions under stimulation and will require further investigation. To achieve this, studies into different biostable inorganic layers as adhesion promoters will aid the manufacture of chronically stable stimulation devices.

Acknowledgements

P.J. would like to acknowledge funding from the EPRSC and Johnson Matthey iCASE studentship (G102881), and the Royal Commission of the Exhibition of 1851 (G106790).

References

[1] D.T. Brocker, W.M. Grill, Principles of electrical stimulation of neural tissue, in: Handbook of Clinical Neurology, Elsevier B.V., 2013: pp. 3–18. https://doi.org/10.1016/B978-0-444-53497-2.00001-2.

[2] F.M. Weaver, K.T. Stroupe, B. Smith, B. Gonzalez, Z. Huo, L. Cao, D. Ippolito, K.A. Follett, Survival in patients with Parkinson's disease after deep brain stimulation or medical management, Movement Disorders. 32 (2017) 1756–1763. https://doi.org/10.1002/mds.27235.

[3] V. Krishna, F. Sammartino, N.K.K. King, R.Q.Y. So, R. Wennberg, Neuromodulation for Epilepsy, Neurosurgery Clinics of North America. 27 (2016) 123–131. https://doi.org/10.1016/j.nec.2015.08.010.

[4] T.E. Schlaepfer, B. Bewernick, Update on Neuromodulation for Treatment-Resistant Depression, F1000Research. 4 (2015). https://doi.org/10.12688/f1000research.6633.1.

[5] N.R. Williams, E.B. Short, T. Hopkins, B.S. Bentzley, G.L. Sahlem, J. Pannu, M. Schmidt, J.J. Borckardt, J.E. Korte, M.S. George, I. Takacs, Z. Nahas, Five-Year Follow-Up of Bilateral Epidural Prefrontal Cortical Stimulation for Treatment-Resistant Depression, Brain Stimulation. 9 (2016) 897–904. https://doi.org/10.1016/j.brs.2016.06.054.

[6] B. Bonaz, V. Sinniger, D. Hoffmann, D. Clarençon, N. Mathieu, C. Dantzer, L. Vercueil, C. Picq, C. Trocmé, P. Faure, J.L. Cracowski, S. Pellissier, Chronic vagus nerve stimulation in Crohn's disease: A 6-month follow-up pilot study, Neurogastroenterology and Motility. 28 (2016) 948–953. https://doi.org/10.1111/nmo.12792.

[7] K.A.B. Lapidus, E.R. Stern, H.A. Berlin, W.K. Goodman, Neuromodulation for Obsessive-Compulsive Disorder, Neurotherapeutics. 11 (2014) 485–495. https://doi.org/10.1007/s13311-014-0287-9.

[8] D. Val-Laillet, E. Aarts, B. Weber, M. Ferrari, V. Quaresima, L.E. Stoeckel, M. Alonso-Alonso, M. Audette, C.H. Malbert, E. Stice, Neuroimaging and neuromodulation approaches to study eating behavior and prevent and treat eating disorders and obesity, NeuroImage: Clinical. 8 (2015) 1–31. https://doi.org/10.1016/j.nicl.2015.03.016.

[9] J. Gardner, A history of deep brain stimulation: Technological innovation and the role of clinical assessment tools, Social Studies of Science. 43 (2013) 707–728. https://doi.org/10.1177/0306312713483678.

[10] J. Ordonez, M. Schuettler, C. Boehler, T. Boretius, T. Stieglitz, Thin films and microelectrode arrays for neuroprosthetics, MRS Bulletin. 37 (2012) 590–598. https://doi.org/10.1557/mrs.2012.117.

[11] J.S. Ordonez, C. Boehler, M. Schuettler, T. Stieglitz, Improved polyimide thin-film electrodes for neural implants, in: Proceedings of the Annual International Conference of the IEEE Engineering in Medicine and Biology Society, EMBS, 2012: pp. 5134–5137. https://doi.org/10.1109/EMBC.2012.6347149.

[12] F. Ceyssens, R. Puers, Insulation lifetime improvement of polyimide thin film neural implants, Journal of Neural Engineering. 12 (2015) 054001. https://doi.org/10.1088/1741-2560/12/5/054001.

[13] J. Pfau, D. Ganatra, A. Weltin, G. Urban, J. Kieninger, T. Stieglitz, Electrochemical Stability of Thin-Film Platinum as Suitable Material for Neural Stimulation Electrodes, in: Proceedings of the Annual International Conference of the IEEE Engineering in Medicine and Biology Society, EMBS, Institute of Electrical and Electronics Engineers Inc., 2019: pp. 3762–3765. https://doi.org/10.1109/EMBC.2019.8856621.

[14] Y. Xu, C. Luo, F.G. Zeng, J.C. Middlebrooks, H.W. Lin, Z. You, Design, fabrication, and evaluation of a parylene thin-film electrode array for cochlear implants, IEEE Transactions on Biomedical Engineering. 66 (2019) 573–583. https://doi.org/10.1109/TBME.2018.2850753.

[15] U.A. Aregueta-Robles, A.J. Woolley, L.A. Poole-Warren, N.H. Lovell, R.A. Green, Organic electrode coatings for next-generation neural interfaces, Frontiers in Neuroengineering. 7 (2014) 15. https://doi.org/10.3389/fneng.2014.00015.

[16] J.D. Weiland, D.J. Anderson, Chronic neural stimulation with thin-film, iridium oxide electrodes, IEEE Transactions on Biomedical Engineering. 47 (2000) 911–918. https://doi.org/10.1109/10.846685.

[17] J.L. Parker, C. Treaba, Thin film fabrication technique for implantable electrodes, 5,720,099, 1996.

[18] T. Araki, L.M. Bongartz, T. Kaiju, A. Takemoto, S. Tsuruta, T. Uemura, T. Sekitani, Flexible neural interfaces for brain implants-The pursuit of thinness and high density, Flexible and Printed Electronics. 5 (2020) 043002. https://doi.org/10.1088/2058-8585/abc3ca.

[19] ISO, ISO 10993-18:2020(en), Biological evaluation of medical devices — Part 18: Chemical characterization of medical device materials within a risk management process, (n.d.). https://www.iso.org/obp/ui/fr/#iso:std:iso:10993:-18:ed-2:v1:en (accessed January 12, 2020).

[20] D.R. Merrill, M. Bikson, J.G.R. Jefferys, Electrical stimulation of excitable tissue: Design of efficacious and safe protocols, Journal of Neuroscience Methods. 141 (2005) 171–198. https://doi.org/10.1016/j.jneumeth.2004.10.020.

[21] M. Ohring, Why are thin films different from the bulk?, in: H.E. Bennett, L.L. Chase, A.H. Guenther, B.E. Newnam, M.J. Soileau (Eds.), Laser-Induced Damage in Optical Materials: 1993, SPIE, 1994: p. 624. https://doi.org/10.1117/12.180875.

[22] J. Delbeke, S. Haesler, D. Prodanov, Failure Modes of Implanted Neural Interfaces, in: Neural Interface Engineering, Springer International Publishing, 2020: pp. 123–172. https://doi.org/10.1007/978-3-030-41854-0_6.

[23] P. Fattahi, G. Yang, G. Kim, M.R. Abidian, A review of organic and inorganic biomaterials for neural interfaces, Advanced Materials. 26 (2014) 1846–1885. https://doi.org/10.1002/adma.201304496.

[24] S.P. Lacour, G. Courtine, J. Guck, Materials and technologies for soft implantable neuroprostheses, Nature Reviews Materials. 1 (2016) 1–14. https://doi.org/10.1038/natrevmats.2016.63.

[25] J.M. Anderson, A. Rodriguez, D.T. Chang, Foreign body reaction to biomaterials, Seminars in Immunology. 20 (2008) 86–100. https://doi.org/10.1016/j.smim.2007.11.004.

[26] S.M. Wellman, J.R. Eles, K.A. Ludwig, J.P. Seymour, N.J. Michelson, W.E. McFadden, A.L. Vazquez, T.D.Y. Kozai, A Materials Roadmap to Functional Neural Interface Design, Advanced Functional Materials. 28 (2018). https://doi.org/10.1002/adfm.201701269.

[27] C.M. Luetje, K. Jackson, Cochlear implants in children: What constitutes a complication?, in: Otolaryngology - Head and Neck Surgery, SAGE Publications Inc., 1997: pp. 243–247. https://doi.org/10.1016/S0194-5998(97)70181-5.

[28] C.J. Bettinger, M. Ecker, T.D. Yoshida Kozai, G.G. Malliaras, E. Meng, W. Voit, Recent advances in neural interfaces - Materials chemistry to clinical translation, MRS Bulletin. 45 (2020) 655–668. https://doi.org/10.1557/mrs.2020.195.

[29] A.P. Burdick, M.S. Okun, I.U. Haq, H.E. Ward, F. Bova, C.E. Jacobson, D. Bowers, P. Zeilman, K.D. Foote, Prevalence of Twiddler's Syndrome as a Cause of Deep Brain Stimulation Hardware Failure, Stereotactic and Functional Neurosurgery. 88 (2010) 353–359. https://doi.org/10.1159/000319039.

[30] M.N. Børretzen, S. Bjerknes, T. Sæhle, M. Skjelland, I.M. Skogseid, M. Toft, E. Dietrichs, Long-term follow-up of thalamic deep brain stimulation for essential tremor - patient satisfaction and mortality, BMC Neurology. 14 (2014) 120. https://doi.org/10.1186/1471-2377-14-120.

[31] M. Gulino, D. Kim, S. Pané, S.D. Santos, A.P. Pêgo, Tissue response to neural implants: The use of model systems toward new design solutions of implantable microelectrodes, Frontiers in Neuroscience. 13 (2019) 689. https://doi.org/10.3389/fnins.2019.00689.

[32] V.S. Polikov, P.A. Tresco, W.M. Reichert, Response of brain tissue to chronically implanted neural electrodes, Journal of Neuroscience Methods. 148 (2005) 1–18. https://doi.org/10.1016/j.jneumeth.2005.08.015.

[33] C. Hassler, T. Boretius, T. Stieglitz, Polymers for neural implants, Journal of Polymer Science, Part B: Polymer Physics. 49 (2011) 18–33. https://doi.org/10.1002/polb.22169.

[34] A.M. Dymond, L.E. Kaechele, J.M. Jurist, P.H. Crandall, Brain tissue reaction to some chronically implanted metals., Journal of Neurosurgery. 33 (1970) 574–580. https://doi.org/10.3171/jns.1970.33.5.0574.

[35] B.J. Kim, J.T.W. Kuo, S.A. Hara, C.D. Lee, L. Yu, C.A. Gutierrez, T.Q. Hoang, V. Pikov, E. Meng, 3D Parylene sheath neural probe for chronic recordings, Journal of Neural Engineering. 10 (2013). https://doi.org/10.1088/1741-2560/10/4/045002.

[36] K.A. Ludwig, J.D. Uram, J. Yang, D.C. Martin, D.R. Kipke, Chronic neural recordings using silicon microelectrode arrays electrochemically deposited with a poly(3,4-ethylenedioxythiophene) (PEDOT) film, Journal of Neural Engineering. 3 (2006) 59–70. https://doi.org/10.1088/1741-2560/3/1/007.

[37] R.J. Vetter, J.C. Williams, J.F. Hetke, E.A. Nunamaker, D.R. Kipke, Chronic neural recording using silicon-substrate microelectrode arrays implanted in cerebral cortex, IEEE Transactions on Biomedical Engineering. 51 (2004) 896–904. https://doi.org/10.1109/TBME.2004.826680.

[38] H.Y. Lai, L. de Liao, C.T. Lin, J.H. Hsu, X. He, Y.Y. Chen, J.Y. Chang, H.F. Chen, S. Tsang, Y.Y.I. Shih, Design, simulation and experimental validation of a novel flexible neural probe for deep

brain stimulation and multichannel recording, Journal of Neural Engineering. 9 (2012). https://doi.org/10.1088/1741-2560/9/3/036001.

[39] X.T. Cui, D.D. Zhou, Poly (3,4-ethylenedioxythiophene) for chronic neural stimulation, IEEE Transactions on Neural Systems and Rehabilitation Engineering. 15 (2007) 502–508. https://doi.org/10.1109/TNSRE.2007.909811.

[40] R. Caldwell, M.G. Street, R. Sharma, P. Takmakov, B. Baker, L. Rieth, Characterization of Parylene-C degradation mechanisms: In vitro reactive accelerated aging model compared to multiyear in vivo implantation, Biomaterials. 232 (2020) 119731. https://doi.org/10.1016/j.biomaterials.2019.119731.

[41] M.A. Lebedev, M.A.L. Nicolelis, Brain-machine interfaces: past, present and future, Trends in Neurosciences. 29 (2006) 536–546. https://doi.org/10.1016/j.tins.2006.07.004.

[42] P.F. Johnson, L.L. Hench, An in vitro analysis of metal electrodes for use in the neural environment, Brain, Behavior and Evolution. 14 (1977) 3–23. https://doi.org/10.1159/000124612.

[43] M.G. Street, C.G. Welle, P.A. Takmakov, Automated reactive accelerated aging for rapid in vitro evaluation of neural implant performance, Review of Scientific Instruments. 89 (2018) 094301. https://doi.org/10.1063/1.5024686.

[44] B. Rubehn, T. Stieglitz, In vitro evaluation of the long-term stability of polyimide as a material for neural implants, Biomaterials. 31 (2010) 3449–3458. https://doi.org/10.1016/j.biomaterials.2010.01.053.

[45] A. Lecomte, A. Degache, E. Descamps, L. Dahan, C. Bergaud, In vitro and in vivo biostability assessment of chronically-implanted Parylene C neural sensors, Sensors and Actuators, B: Chemical. 251 (2017) 1001–1008. https://doi.org/10.1016/j.snb.2017.05.057.

[46] S. Bredeson, A. Kanneganti, F. Deku, S. Cogan, M. Romero-Ortega, P. Troyk, Chronic in-vivo testing of a 16-channel implantable wireless neural stimulator, in: Proceedings of the Annual International Conference of the IEEE Engineering in Medicine and Biology Society, EMBS, Institute of Electrical and Electronics Engineers Inc., 2015: pp. 1017–1020. https://doi.org/10.1109/EMBC.2015.7318537.

[47] A. Prasad, J.C. Sanchez, Quantifying long-term microelectrode array functionality using chronic in vivo impedance testing, Journal of Neural Engineering. 9 (2012) 026028. https://doi.org/10.1088/1741-2560/9/2/026028.

[48] S. Löffler, Y. Xie, P. Klimach, A. Richter, P. Detemple, T. Stieglitz, A. Moser, U.G. Hofmann, Long term in vivo stability and frequency response of polyimide based flexible array probes, Biomedizinische Technik. 57 (2012) 104–107. https://doi.org/10.1515/bmt-2012-4434.

[49] J.C. Barrese, J. Aceros, J.P. Donoghue, Scanning electron microscopy of chronically implanted intracortical microelectrode arrays in non-human primates, Journal of Neural Engineering. 13 (2016) 026003. https://doi.org/10.1088/1741-2560/13/2/026003.

[50] R. Daschner, U. Greppmaier, M. Kokelmann, S. Rudorf, R. Rudorf, S. Schleehauf, W.G. Wrobel, Laboratory and clinical reliability of conformally coated subretinal implants, Biomedical Microdevices. 19 (2017) 7. https://doi.org/10.1007/s10544-017-0147-6.

[51] J.A. George, D.M. Page, T.S. Davis, C.C. Duncan, D.T. Hutchinson, L.W. Rieth, G.A. Clark, Long-term performance of Utah slanted electrode arrays and intramuscular electromyographic leads implanted chronically in human arm nerves and muscles, Journal of Neural Engineering. 17 (2020) 056042. https://doi.org/10.1088/1741-2552/abc025.

[52] J.C. Barrese, N. Rao, K. Paroo, C. Triebwasser, C. Vargas-Irwin, L. Franquemont, J.P. Donoghue, Failure mode analysis of silicon-based intracortical microelectrode arrays in non-human primates, Journal of Neural Engineering. 10 (2013) 066014. https://doi.org/10.1088/1741-2560/10/6/066014.

[53] G. Agarwal, A.A. Wilfong, J.L. Edmonds, Surgical revision of vagus nerve stimulation electrodes in children, Otolaryngology - Head and Neck Surgery. 144 (2011) 123–124. https://doi.org/10.1177/0194599810390896.

[54] P. Blomstedt, M.I. Hariz, Hardware-related complications of deep brain stimulation: A ten year experience, Acta Neurochirurgica. 147 (2005) 1061–1064. https://doi.org/10.1007/s00701-005-0576-5.

[55] A.N. Dalrymple, U.A. Robles, M. Huynh, B.A. Nayagam, R.A. Green, L.A. Poole-Warren, J.B. Fallon, R.K. Shepherd, Electrochemical and biological performance of chronically stimulated conductive hydrogel electrodes, J. Neural Eng. 17 (2020) 26018. https://doi.org/10.1088/1741-2552/ab7cfc.

[56] N. Lago, K. Yoshida, K.P. Koch, X. Navarro, Assessment of biocompatibility of chronically implanted polyimide and platinum intrafascicular electrodes, IEEE Transactions on Biomedical Engineering. 54 (2007) 281–290. https://doi.org/10.1109/TBME.2006.886617.

[57] P.E.K. Donaldson, N. de N. Donaldson, G.S. Brindley, Life of Pt and Pt-Ir stimulating electrodes in neurological prostheses, Medical & Biological Engineering & Computing. 23 (1985) 84–86. https://doi.org/10.1007/BF02444034.

[58] B.K. Shepherd, G.M. Clark, Scanning electron microscopy of platinum scala tympani electrodes following chronic stimulation in patients, Biomaterials. 12 (1991) 417–423. https://doi.org/10.1016/0142-9612(91)90011-X.

[59] A.S. Pranti, A. Schander, A. Bödecker, W. Lang, Highly Stable PEDOT:PSS Coating on Gold Microelectrodes with Improved Charge Injection Capacity for Chronic Neural Stimulation, Proceedings. 1 (2017) 492. https://doi.org/10.3390/proceedings1040492.

[60] D.A.X. Nayagam, R.A. Williams, P.J. Allen, M.N. Shivdasani, C.D. Luu, C.M. Salinas-LaRosa, S. Finch, L.N. Ayton, A.L. Saunders, M. McPhedran, C. McGowan, J. Villalobos, J.B. Fallon, A.K. Wise, J. Yeoh, J. Xu, H. Feng, R. Millard, M. McWade, P.C. Thien, C.E. Williams, R.K. Shepherd, Chronic Electrical Stimulation with a Suprachoroidal Retinal Prosthesis: A Preclinical Safety and Efficacy Study, PLoS ONE. 9 (2014) e97182. https://doi.org/10.1371/journal.pone.0097182.

[61] C. Boehler, D.M. Vieira, U. Egert, M. Asplund, NanoPt - A Nanostructured Electrode Coating for Neural Recording and Microstimulation, ACS Applied Materials and Interfaces. 12 (2020) 14855–14865. https://doi.org/10.1021/acsami.9b22798.

[62] P. Čvančara, T. Boretius, V.M. López-Ɔ lvarez, P. Maciejasz, D. Andreu, S. Raspopovic, F. Petrini, S. Micera, G. Granata, E. Fernandez, P.M. Rossini, K. Yoshida, W. Jensen, J.L. Divoux, D. Guiraud, X. Navarro, T. Stieglitz, Stability of flexible thin-film metallization stimulation

electrodes: Analysis of explants after first-in-human study and improvement of in vivo performance, Journal of Neural Engineering. 17 (2020) 46006. https://doi.org/10.1088/1741-2552/ab9a9a.

[63] G. Schiavone, X. Kang, F. Fallegger, J. Gandar, G. Courtine, S.P. Lacour, Guidelines to Study and Develop Soft Electrode Systems for Neural Stimulation, Neuron. 108 (2020) 238–258. https://doi.org/10.1016/j.neuron.2020.10.010.

[64] C. Boehler, S. Carli, L. Fadiga, T. Stieglitz, M. Asplund, Tutorial: guidelines for standardized performance tests for electrodes intended for neural interfaces and bioelectronics, Nature Protocols. 15 (2020) 3557–3578. https://doi.org/10.1038/s41596-020-0389-2.

[65] D.W.L. Hukins, A. Mahomed, S.N. Kukureka, Accelerated aging for testing polymeric biomaterials and medical devices, Medical Engineering & Physics. 30 (2008) 1270–1274. https://doi.org/10.1016/j.medengphy.2008.06.001.

[66] H. Hämmerle, K. Kobuch, K. Kohler, W. Nisch, H. Sachs, M. Stelzle, Biostability of micro-photodiode arrays for subretinal implantation, Biomaterials. 23 (2002) 797–804. https://doi.org/10.1016/S0142-9612(01)00185-5.

[67] G. Dijk, A.L. Rutz, G.G. Malliaras, Stability of PEDOT:PSS-Coated Gold Electrodes in Cell Culture Conditions, Advanced Materials Technologies. 5 (2020) 1900662. https://doi.org/10.1002/admt.201900662.

[68] S.F. Cogan, Neural Stimulation and Recording Electrodes, Annual Review of Biomedical Engineering. 10 (2008) 275–309. https://doi.org/10.1146/annurev.bioeng.10.061807.160518.

[69] B. Rubehn, C. Bosman, R. Oostenveld, P. Fries, T. Stieglitz, A MEMS-based flexible multichannel ECoG-electrode array, Journal of Neural Engineering. 6 (2009) 036003. https://doi.org/10.1088/1741-2560/6/3/036003.

[70] R. v. Shannon, A Model of Safe Levels for Electrical Stimulation, IEEE Transactions on Biomedical Engineering. 39 (1992) 424–426. https://doi.org/10.1109/10.126616.

[71] S.F. Cogan, D.J. Garrett, R.A. Green, Electrochemical Principles of Safe Charge Injection, in: Neurobionics: The Biomedical Engineering of Neural Prostheses, John Wiley & Sons, Inc., Hoboken, NJ, USA, 2016: pp. 55–88. https://doi.org/10.1002/9781118816028.ch3.

[72] G. Kook, S.W. Lee, H.C. Lee, I.J. Cho, H.J. Lee, Neural probes for chronic applications, Micromachines. 7 (2016) 179. https://doi.org/10.3390/mi7100179.

[73] D.R. Kipke, W. Shain, G. Buzsáki, E. Fetz, J.M. Henderson, J.F. Hetke, G. Schalk, Advanced neurotechnologies for chronic neural interfaces: New horizons and clinical opportunities, in: Journal of Neuroscience, Society for Neuroscience, 2008: pp. 11830–11838. https://doi.org/10.1523/JNEUROSCI.3879-08.2008.

[74] C. Günter, J. Delbeke, M. Ortiz-Catalan, Safety of long-term electrical peripheral nerve stimulation: review of the state of the art, (n.d.). https://doi.org/10.1186/s12984-018-0474-8.

[75] J.C. Lilly, J.R. Hughes, E.C. Alvord, T.W. Galkin, Brief, noninjurious electric waveform for stimulation of the brain, Science. 121 (1955) 468–469. https://doi.org/10.1126/science.121.3144.468.

[76] R.T. Leung, M.N. Shivdasani, D.A.X. Nayagam, R.K. Shepherd, In vivo and in vitro comparison of the charge injection capacity of platinum macroelectrodes, IEEE Transactions on Biomedical Engineering. 62 (2015) 849–857. https://doi.org/10.1109/TBME.2014.2366514.

[77] J. McHardy, L.S. Robblee, J.M. Marston, S.B. Brummer, Electrical stimulation with Pt electrodes. IV. Factors influencing Pt dissolution in inorganic saline, Biomaterials. 1 (1980) 129–134. https://doi.org/10.1016/0142-9612(80)90034-4.

[78] Z. Hu, P.R. Troyk, T.P. Brawn, D. Margoliash, S.F. Cogan, In Vitro and in Vivo charge capacity of AIROF microelectrodes, in: Annual International Conference of the IEEE Engineering in Medicine and Biology - Proceedings, Conf Proc IEEE Eng Med Biol Soc, 2006: pp. 886–889. https://doi.org/10.1109/IEMBS.2006.259869.

[79] A.S. Pranti, A. Schander, A. Bödecker, W. Lang, PEDOT: PSS coating on gold microelectrodes with excellent stability and high charge injection capacity for chronic neural interfaces, Sensors and Actuators, B: Chemical. 275 (2018) 382–393. https://doi.org/10.1016/j.snb.2018.08.007.

[80] O.O. Abegunde, E.T. Akinlabi, O.P. Oladijo, S. Akinlabi, A.U. Ude, Overview of thin film deposition techniques, (2019). https://doi.org/10.3934/matersci.2019.2.174.

[81] D. Khodagholy, J.N. Gelinas, T. Thesen, W. Doyle, O. Devinsky, G.G. Malliaras, G. Buzsáki, NeuroGrid: Recording action potentials from the surface of the brain, Nature Neuroscience. 18 (2015) 310–315. https://doi.org/10.1038/nn.3905.

[82] D. Khodagholy, T. Doublet, M. Gurfinkel, P. Quilichini, E. Ismailova, P. Leleux, T. Herve, S. Sanaur, C. Bernard, G.G. Malliaras, Highly Conformable Conducting Polymer Electrodes for In Vivo Recordings, Advanced Materials. 23 (2011) H268–H272. https://doi.org/10.1002/adma.201102378.

[83] S. Myllymaa, K. Myllymaa, R. Lappalaine, Flexible Implantable Thin Film Neural Electrodes, in: Recent Advances in Biomedical Engineering, InTech, 2009. https://doi.org/10.5772/7479.

[84] C.D. Lee, E. Meng, Mechanical Properties of Thin-Film Parylene–Metal–Parylene Devices, Frontiers in Mechanical Engineering. 1 (2015). https://doi.org/10.3389/fmech.2015.00010.

[85] J. Li, Biofluid Barrier Materials and Encapsulation Strategies for Flexible, Chronically Stable Neural Interfaces, in: Neural Interface Engineering, Springer International Publishing, 2020: pp. 267–280. https://doi.org/10.1007/978-3-030-41854-0_10.

[86] J.C. Barrese, N. Rao, K. Paroo, C. Triebwasser, C. Vargas-Irwin, L. Franquemont, J.P. Donoghue, Failure mode analysis of silicon-based intracortical microelectrode arrays in non-human primates, Journal of Neural Engineering. 10 (2013). https://doi.org/10.1088/1741-2560/10/6/066014.

[87] R.K. Shepherd, J. Villalobos, O. Burns, D.A.X. Nayagam, The development of neural stimulators: A review of preclinical safety and efficacy studies, Journal of Neural Engineering. 15 (2018) 041004. https://doi.org/10.1088/1741-2552/aac43c.

[88] H. Fang, J. Zhao, K.J. Yu, E. Song, A.B. Farimani, C.-H. Chiang, X. Jin, Y. Xue, D. Xu, W. Du, K.J. Seo, Y. Zhong, Z. Yang, S.M. Won, G. Fang, S.W. Choi, S. Chaudhuri, Y. Huang, M.A. Alam, J. Viventi, N.R. Aluru, J.A. Rogers, Ultrathin, transferred layers of thermally grown silicon dioxide

as biofluid barriers for biointegrated flexible electronic systems, PNAS. 113 (2016) 11682–11687. https://doi.org/10.1073/pnas.1605269113.

[89] R. Feiner, L. Engel, S. Fleischer, M. Malki, I. Gal, A. Shapira, Y. Shacham-Diamand, T. Dvir, Engineered hybrid cardiac patches with multifunctional electronics for online monitoring and regulation of tissue function, Nature Materials. 15 (2016) 679–685. https://doi.org/10.1038/nmat4590.

[90] J. Li, E. Song, C.H. Chiang, K.J. Yu, J. Koo, H. Du, Y. Zhong, M. Hill, C. Wang, J. Zhang, Y. Chen, L. Tian, Y. Zhong, G. Fanga, J. Vivent, J.A. Rogers, Conductively coupled flexible silicon electronic systems for chronic neural electrophysiology, Proceedings of the National Academy of Sciences of the United States of America. 115 (2018) E9542–E9549. https://doi.org/10.1073/pnas.1813187115.

[91] G.B. Alexander, W.M. Heston, R.K. Iler, The solubility of amorphous silica in water, Journal of Physical Chemistry. 58 (1954) 453–455. https://doi.org/10.1021/j150516a002.

[92] M.D. Groner, S.M. George, R.S. McLean, P.F. Carcia, Gas diffusion barriers on polymers using Al 2 O 3 atomic layer deposition, Applied Physics Letters. 88 (2006) 1–3. https://doi.org/10.1063/1.2168489.

[93] M. Velderrain, Designing low permeability, optical-grade silicone systems: guidelines for choosing a silicone based on transmission rates for barrier applications, in: L.-C. Chien, S.-D. Lee, M.H. Wu (Eds.), Advances in Display Technologies II, SPIE, 2012: p. 82800O. https://doi.org/10.1117/12.910642.

[94] A. Hogg, S. Uhl, F. Feuvrier, Y. Girardet, B. Graf, T. Aellen, H. Keppner, Y. Tardy, J. Burger, Protective multilayer packaging for long-term implantable medical devices, Surface and Coatings Technology. 255 (2014) 124–129. https://doi.org/10.1016/j.surfcoat.2014.02.070.

[95] T. Stieglitz, H. Beutel, M. Schuettler, J.U. Meyer, Micromachined, polyimide-based devices for flexible neural interfaces, Biomedical Microdevices. 2 (2000) 283–294. https://doi.org/10.1023/A:1009955222114.

[96] Seung Woo Lee, Kyou Sik Min, Joonsoo Jeong, Junghoon Kim, Sung June Kim, Monolithic Encapsulation of Implantable Neuroprosthetic Devices Using Liquid Crystal Polymers, IEEE Transactions on Biomedical Engineering. 58 (2011) 2255–2263. https://doi.org/10.1109/TBME.2011.2136341.

[97] N. de La Oliva, M. Mueller, T. Stieglitz, X. Navarro, J. del Valle, On the use of Parylene C polymer as substrate for peripheral nerve electrodes, Scientific Reports. 8 (2018). https://doi.org/10.1038/s41598-018-24502-z.

[98] J. Ortigoza-Diaz, K. Scholten, C. Larson, A. Cobo, T. Hudson, J. Yoo, A. Baldwin, A.W. Hirschberg, E. Meng, Techniques and considerations in the microfabrication of parylene c microelectromechanical systems, Micromachines. 9 (2018). https://doi.org/10.3390/mi9090422.

[99] J. Ortigoza-DIaz, K. Scholten, E. Meng, Characterization and Modification of Adhesion in Dry and Wet Environments in Thin-Film Parylene Systems, Journal of Microelectromechanical Systems. 27 (2018) 874–885. https://doi.org/10.1109/JMEMS.2018.2854636.

[100] J. Jeong, K.S. Min, S.J. Kim, Microfabrication process for long-term reliable neural electrode arrays using liquid crystal polymer (LCP), Microelectronic Engineering. 216 (2019) 111096. https://doi.org/10.1016/j.mee.2019.111096.

[101] S.H. Huang, S.P. Lin, J.J.J. Chen, In vitro and in vivo characterization of SU-8 flexible neuroprobe: From mechanical properties to electrophysiological recording, Sensors and Actuators, A: Physical. 216 (2014) 257–265. https://doi.org/10.1016/j.sna.2014.06.005.

[102] A. Altuna, L. Menendez de la Prida, E. Bellistri, G. Gabriel, A. Guimerá, J. Berganzo, R. Villa, L.J. Fernández, SU-8 based microprobes with integrated planar electrodes for enhanced neural depth recording, Biosensors and Bioelectronics. 37 (2012) 1–5. https://doi.org/10.1016/j.bios.2012.03.039.

[103] M. Kaltenbrunner, T. Sekitani, J. Reeder, T. Yokota, K. Kuribara, T. Tokuhara, M. Drack, R. Schwödiauer, I. Graz, S. Bauer-Gogonea, S. Bauer, T. Someya, An ultra-lightweight design for imperceptible plastic electronics, Nature. 499 (2013) 458–463. https://doi.org/10.1038/nature12314.

[104] N. Kunori, I. Takashima, A transparent epidural electrode array for use in conjunction with optical imaging, Journal of Neuroscience Methods. 251 (2015) 130–137. https://doi.org/10.1016/j.jneumeth.2015.05.018.

[105] M. Cabello, C. Aracil, F. Perdigones, M. Mozo, B. de la Cerda, J.M. Quero, Gold microelectrodes array embedded in PDMS for electrical stimulation and signal detection, Sensors and Actuators, B: Chemical. 257 (2018) 954–962. https://doi.org/10.1016/j.snb.2017.11.026.

[106] L. Guo, G.S. Guvanasen, X. Liu, C. Tuthill, T.R. Nichols, S.P. Deweerth, A PDMS-based integrated stretchable microelectrode array (isMEA) for neural and muscular surface interfacing, IEEE Transactions on Biomedical Circuits and Systems. 7 (2013) 1–10. https://doi.org/10.1109/TBCAS.2012.2192932.

[107] J.H.C. Chang, Y. Liu, Y.C. Tai, Long term glass-encapsulated packaging for implant electronics, in: Proceedings of the IEEE International Conference on Micro Electro Mechanical Systems (MEMS), Institute of Electrical and Electronics Engineers Inc., 2014: pp. 1127–1130. https://doi.org/10.1109/MEMSYS.2014.6765844.

[108] S. Minnikanti, G. Diao, J.J. Pancrazio, X. Xie, L. Rieth, F. Solzbacher, N. Peixoto, Lifetime assessment of atomic-layer-deposited Al2O3–Parylene C bilayer coating for neural interfaces using accelerated age testing and electrochemical characterization, Acta Biomaterialia. 10 (2014) 960–967. https://doi.org/10.1016/j.actbio.2013.10.031.

[109] B.F.E. Matarèse, P.L.C. Feyen, A. Falco, F. Benfenati, P. Lugli, J.C. Demello, Use of SU8 as a stable and biocompatible adhesion layer for gold bioelectrodes, Scientific Reports. 8 (2018) 1–12. https://doi.org/10.1038/s41598-018-21755-6.

[110] T. Sekitani, T. Yokota, K. Kuribara, M. Kaltenbrunner, T. Fukushima, Y. Inoue, M. Sekino, T. Isoyama, Y. Abe, H. Onodera, T. Someya, Ultraflexible organic amplifier with biocompatible gel electrodes, Nature Communications. 7 (2016) 1–11. https://doi.org/10.1038/ncomms11425.

[111] Y. Poojari, Silicones for Encapsulation of Medical Device Implants, Silicon. 9 (2017) 645–649. https://doi.org/10.1007/s12633-017-9603-4.

[112] J. Jeong, S. Hyun Bae, J.M. Seo, H. Chung, S. June Kim, Long-term evaluation of a liquid crystal polymer (LCP)-based retinal prosthesis, Journal of Neural Engineering. 13 (2016) 025004. https://doi.org/10.1088/1741-2560/13/2/025004.

[113] R.L. White, T.J. Gross, An Evaluation of the Resistance to Electrolysis of Metals for Use in Biostimulation Microprobes, IEEE Transactions on Biomedical Engineering. BME-21 (1974) 487–490. https://doi.org/10.1109/TBME.1974.324339.

[114] A.B. Majji, M.S. Humayun, J.D. Weiland, S. Suzuki, S.A. D'Anna, E. de Juan, Long-term histological and electrophysiological results of an inactive epiretinal electrode array implantation in dogs, Investigative Ophthalmology and Visual Science. 40 (1999) 2073–2081. https://europepmc.org/article/med/10440263 (accessed January 5, 2021).

[115] C.H. Chouard, P. Pialoux, [Biocompatibility of cochlear implants]., Bulletin de l'Academie nationale de medecine. 179 (1995) 549–555.

[116] K. Wissel, G. Brandes, N. Pütz, G.L. Angrisani, J. Thieleke, T. Lenarz, M. Durisin, Platinum corrosion products from electrode contacts of human cochlear implants induce cell death in cell culture models, PLOS ONE. 13 (2018) e0196649. https://doi.org/10.1371/journal.pone.0196649.

[117] K.M. Kovach, D.W. Kumsa, V. Srivastava, E.M. Hudak, D.F. Untereker, S.C. Kelley, H.A. von Recum, J.R. Capadona, High-throughput in vitro assay to evaluate the cytotoxicity of liberated platinum compounds for stimulating neural electrodes, Journal of Neuroscience Methods. 273 (2016) 1–9. https://doi.org/10.1016/j.jneumeth.2016.07.018.

[118] R.K. Shepherd, P. Carter, A. Dalrymple, Y.L. Enke, A.K. Wise, T. Nguyen, J. Firth, A. Thompson, J.B. Fallon, Platinum dissolution and tissue response following long-term electrical stimulation at high charge densities, Journal of Neural Engineering. (2021). https://doi.org/10.1088/1741-2552/abe5ba.

[119] N. Eliaz, Corrosion of metallic biomaterials: A review, Materials. 12 (2019). https://doi.org/10.3390/ma12030407.

[120] R.A. Frederick, I.Y. Meliane, A. Joshi-Imre, P.R. Troyk, S.F. Cogan, Activated iridium oxide film (AIROF) electrodes for neural tissue stimulation, Journal of Neural Engineering. 17 (2020) 56001. https://doi.org/10.1088/1741-2552/abb9bf.

[121] A. Frommhold, E. Tarte, Effect of film structure on the electrochemical properties of gold electrodes for neural implants, Electrochimica Acta. 56 (2011) 6001–6007. https://doi.org/10.1016/j.electacta.2011.04.100.

[122] F. Rodrigues, J.F. Ribeiro, P.A. Anacleto, A. Fouchard, O. David, P.M. Sarro, P.M. Mendes, Fabrication and characterization of polyimide-based "smooth" titanium nitride microelectrode arrays for neural stimulation and recording, in: Journal of Neural Engineering, Institute of Physics Publishing, 2020: p. 016010. https://doi.org/10.1088/1741-2552/ab4dbb.

[123] M. Vomero, E. Castagnola, J.S. Ordonez, S. Carli, E. Zucchini, E. Maggiolini, C. Gueli, N. Goshi, F. Ciarpella, C. Cea, L. Fadiga, D. Ricci, S. Kassegne, T. Stieglitz, Incorporation of Silicon Carbide and Diamond-Like Carbon as Adhesion Promoters Improves In Vitro and In Vivo Stability of Thin-Film Glassy Carbon Electrocorticography Arrays, Advanced Biosystems. 2 (2018) 1700081. https://doi.org/10.1002/adbi.201700081.

[124] M. Ganji, A. Tanaka, V. Gilja, E. Halgren, S.A. Dayeh, Scaling Effects on the Electrochemical Stimulation Performance of Au, Pt, and PEDOT:PSS Electrocorticography Arrays, Advanced Functional Materials. 27 (2017) 1703019. https://doi.org/10.1002/adfm.201703019.

[125] M. Wood, R.K. Willits, Short-duration, DC electrical stimulation increases chick embryo DRG neurite outgrowth, Bioelectromagnetics. 27 (2006) 328–331. https://doi.org/10.1002/bem.20214.

[126] C.D. McCaig, Nerve growth in the absence of growth cone filopodia and the effects of a small applied electric field, Journal of Cell Science. 93 (1989) 715–721.

[127] A.C. Mendonça, C.H. Barbieri, N. Mazzer, Directly applied low intensity direct electric current enhances peripheral nerve regeneration in rats., Journal of Neuroscience Methods. 129 (2003) 183–90. https://doi.org/10.1016/s0165-0270(03)00207-3.

[128] B. Song, M. Zhao, J. Forrester, C. McCaig, Nerve regeneration and wound healing are stimulated and directed by an endogenous electrical field in vivo, Journal of Cell Science. 117 (2004) 4681–4690. https://doi.org/10.1242/jcs.01341.

[129] Y.J. Chang, C.M. Hsu, C.H. Lin, M.S.C. Lu, L. Chen, Electrical stimulation promotes nerve growth factor-induced neurite outgrowth and signaling, Biochimica et Biophysica Acta - General Subjects. 1830 (2013) 4130–4136. https://doi.org/10.1016/j.bbagen.2013.04.007.

[130] K.-A. Kim, K. Ja, S. Lee, S. Kim, Biphasic Electrical Currents Stimulation Promotes both Proliferation and Differentiation of Fetal Neural Stem Cells, PLoS ONE. 6 (2011) 18738. https://doi.org/10.1371/journal.pone.0018738.

[131] R.A. Green, N.H. Lovell, G.G. Wallace, L.A. Poole-Warren, Conducting polymers for neural interfaces: Challenges in developing an effective long-term implant, Biomaterials. 29 (2008) 3393–3399. https://doi.org/10.1016/j.biomaterials.2008.04.047.

[132] E. Cuttaz, J. Goding, C. Vallejo-Giraldo, U. Aregueta-Robles, N. Lovell, D. Ghezzi, R.A. Green, Conductive elastomer composites for fully polymeric, flexible bioelectronics, Biomaterials Science. 7 (2019) 1372–1385. https://doi.org/10.1039/c8bm01235k.

[133] A. Weltman, J. Yoo, E. Meng, Flexible, penetrating brain probes enabled by advances in polymer microfabrication, Micromachines. 7 (2016). https://doi.org/10.3390/mi7100180.

[134] S. Murray, C. Hillman, M. Pecht, Environmental aging and deadhesion of polyimide dielectric films, Journal of Electronic Packaging, Transactions of the ASME. 126 (2004) 390–397. https://doi.org/10.1115/1.1773853.

[135] J.S. Ordonez, C. Boehler, M. Schuettler, T. Stieglitz, Long-term adhesion studies of polyimide to inorganic and metallic layers, in: Materials Research Society Symposium Proceedings, Cambridge University Press, 2012: pp. 7–13. https://doi.org/10.1557/opl.2012.1198.

[136] D.C. Rodger, A.J. Fong, W. Li, H. Ameri, A.K. Ahuja, C. Gutierrez, I. Lavrov, H. Zhong, P.R. Menon, E. Meng, J.W. Burdick, R.R. Roy, V.R. Edgerton, J.D. Weiland, M.S. Humayun, Y.C. Tai, Flexible parylene-based multielectrode array technology for high-density neural stimulation and recording, Sensors and Actuators, B: Chemical. 132 (2008) 449–460. https://doi.org/10.1016/j.snb.2007.10.069.

[137] R.P. von Metzen, T. Stieglitz, The effects of annealing on mechanical, chemical, and physical properties and structural stability of Parylene C, Biomedical Microdevices. 15 (2013) 727–735. https://doi.org/10.1007/s10544-013-9758-8.

[138] P. Ledochowitsch, R.F. Tiefenauer, B. Pepin, M.M. Maharbiz, T.J. Blanche, Nanoflex for neural nanoprobes, in: 2013 Transducers and Eurosensors XXVII: The 17th International Conference on Solid-State Sensors, Actuators and Microsystems, TRANSDUCERS and EUROSENSORS 2013, 2013: pp. 1278–1281. https://doi.org/10.1109/Transducers.2013.6627009.

[139] FDA/MAUDE, MAUDE - Manufacturer and User Facility Device Experience: citric acid irrigation, 2016. https://www.accessdata.fda.gov/scripts/cdrh/cfdocs/cfMAUDE/search.CFM (accessed January 5, 2021).

[140] R.R. Tambyraja, M.A. Gutman, C.A. Megerian, Cochlear implant complications: Utility of federal database in systematic analysis, Archives of Otolaryngology - Head and Neck Surgery. 131 (2005) 245–250. https://doi.org/10.1001/archotol.131.3.245.

[141] J.C. Barrese, J. Aceros, J.P. Donoghue, Scanning electron microscopy of chronically implanted intracortical microelectrode arrays in non-human primates, Journal of Neural Engineering. 13 (2016) 026003. https://doi.org/10.1088/1741-2560/13/2/026003.

[142] A. Prasad, Q.-S. Xue, R. Dieme, V. Sankar, R.C. Mayrand, T. Nishida, W.J. Streit, J.C. Sanchez, Abiotic-biotic characterization of Pt/Ir microelectrode arrays in chronic implants, Frontiers in Neuroengineering. 7 (2014) 2. https://doi.org/10.3389/fneng.2014.00002.

[143] G.P. Crawford, Flexible Flat Panel Displays, John Wiley & Sons, Ltd, Chichester, UK, 2005. https://doi.org/10.1002/0470870508.

[144] I.-C. Cheng, S. Wagner, Overview of Flexible Electronics Technology, in: W.S., S.A. Wong (Ed.), Flexible Electronics, 2009: pp. 1–28. https://doi.org/10.1007/978-0-387-74363-9_1.

[145] Z. Suo, E.Y. Ma, H. Gleskova, S. Wagner, Mechanics of rollable and foldable film-on-foil electronics, Applied Physics Letters. 74 (1999) 1177–1179. https://doi.org/10.1063/1.123478.

[146] S.P. Lacour, S. Benmerah, E. Tarte, J. Fitzgerald, J. Serra, S. McMahon, J. Fawcett, O. Graudejus, Z. Yu, B. Morrison, Flexible and stretchable micro-electrodes for in vitro and in vivo neural interfaces, Medical and Biological Engineering and Computing. 48 (2010) 945–954. https://doi.org/10.1007/s11517-010-0644-8.

[147] V. Radun, R.P. von Metzen, T. Stieglitz, V. Bucher, A. Stett, Evaluation of adhesion promoters for Parylene C on gold metallization, Current Directions in Biomedical Engineering. 1 (2015) 493–497. https://doi.org/10.1515/cdbme-2015-0118.

[148] R. Waack, N.H. Alex, H.L. Frisch, V. Stannett, M. Szwarc, Permeability of Polymer Films to Gases and Vapors, Industrial & Engineering Chemistry. 47 (1955) 2524–2527. https://doi.org/10.1021/ie50552a045.

[149] S. Marais, Q.T. Nguyen, C. Devallencourt, M. Metayer, T.U. Nguyen, P. Schaetzel, Permeation of water through polar and nonpolar polymers and copolymers: Determination of the concentration-dependent diffusion coefficient, Journal of Polymer Science Part B: Polymer Physics. 38 (2000) 1998–2008. https://doi.org/10.1002/1099-0488(20000801)38:15<1998::AID-POLB50>3.0.CO;2-A.

[150] W. Li, D.C. Rodger, E. Meng, J.D. Weiland, M.S. Humayun, Y.C. Tai, Wafer-level parylene packaging with integrated rf electronics for wireless retinal prostheses, Journal of Microelectromechanical Systems. 19 (2010) 735–742. https://doi.org/10.1109/JMEMS.2010.2049985.

[151] P.J. Rousche, D.S. Pellinen, D.P. Pivin, J.C. Williams, R.J. Vetter, D.R. Kipke, Flexible polyimide-based intracortical electrode arrays with bioactive capability, IEEE Transactions on Biomedical Engineering. 48 (2001) 361–370. https://doi.org/10.1109/10.914800.

[152] S.D. Stoney, W.D. Thompson, H. Asanuma, Excitation of pyramidal tract cells by intracortical microstimulation: effective extent of stimulating current., Journal of Neurophysiology. 31 (1968) 659–669. https://doi.org/10.1152/jn.1968.31.5.659.

[153] M. Modarresi, A. Mehandzhiyski, M. Fahlman, K. Tybrandt, I. Zozoulenko, Microscopic Understanding of the Granular Structure and the Swelling of PEDOT:PSS, (2020). https://doi.org/10.1021/acs.macromol.0c00877.

[154] B. Sarkar, M. Jaiswal, D.K. Satapathy, Swelling kinetics and electrical charge transport in PEDOT:PSS thin films exposed to water vapor, Journal of Physics Condensed Matter. 30 (2018) 225101. https://doi.org/10.1088/1361-648X/aabe51.

[155] L. Bießmann, L.P. Kreuzer, T. Widmann, N. Hohn, J.-F.O. Moulin, P. Mü Ller-Buschbaum, Monitoring the Swelling Behavior of PEDOT:PSS Electrodes under High Humidity Conditions, (2018). https://doi.org/10.1021/acsami.8b00446.

[156] J. Pfau, J.A. Leal Ordonez, T. Stieglitz, In Situ Measurement of Stimulus Induced pH Changes Using ThinFilm Embedded IrOx pH Electrodes, in: Proceedings of the Annual International Conference of the IEEE Engineering in Medicine and Biology Society, EMBS, Institute of Electrical and Electronics Engineers Inc., 2018: pp. 5049–5052. https://doi.org/10.1109/EMBC.2018.8513441.

[157] M. Yu, X. Feng, Thin-Film Electrode-Based Supercapacitors, Joule. 3 (2019) 338–360. https://doi.org/10.1016/j.joule.2018.12.012.

[158] J.R. Aggas, A. Bhat, B.K. Walther, A. Guiseppi-Elie, Nano-Pt ennobling of stainless steel for biomedical applications, Electrochimica Acta. 301 (2019) 153–161. https://doi.org/10.1016/j.electacta.2019.01.177.

[159] M.J. Embleton, The Macrophage (2nd Edn), British Journal of Cancer. 89 (2003) 421–421. https://doi.org/10.1038/sj.bjc.6601103.

[160] G.C. McConnell, H.D. Rees, A.I. Levey, C.A. Gutekunst, R.E. Gross, R. v. Bellamkonda, Implanted neural electrodes cause chronic, local inflammation that is correlated with local neurodegeneration, Journal of Neural Engineering. 6 (2009) 056003. https://doi.org/10.1088/1741-2560/6/5/056003.

[161] S.L. Morton, M. Daroux, J.T. Mortimer, The role of oxygen reduction in electrical stimulation of nervous tissue, in: Proceedings of the Annual Conference on Engineering in Medicine and Biology, Publ by IEEE, 1991: pp. 552–553. https://doi.org/10.1149/1.2054671.

[162] S.B. Brummer, J. McHardy, M.J. Turner, Electrical stimulation with pt electrodes: Trace analysis for dissolved platinum and other dissolved electrochemical products1, Brain, Behavior and Evolution. 14 (1977) 10–22. https://doi.org/10.1159/000124611.

[163] R.C. Black, P. Hannaker, Dissolution of smooth platinum electrodes in biological fluids, Stereotactic and Functional Neurosurgery. 42 (1979) 366–374. https://doi.org/10.1159/000102382.

[164] L.S. Robblee, J. McHardy, J.M. Marston, S.B. Brummer, Electrical stimulation with Pt electrodes. V. The effect of protein on Pt dissolution, Biomaterials. 1 (1980) 135–139. https://doi.org/10.1016/0142-9612(80)90035-6.

[165] L.S. Robblee, J.L. Lefko, S.B. Brummer, Activated Ir: An Electrode Suitable for Reversible Charge Injection in Saline Solution, Journal of The Electrochemical Society. 130 (1983) 731–733. https://doi.org/10.1149/1.2119793.

[166] B. Rosenberg, B. Rosenberg, Some biological effects of platinum compounds: new agents for the control of tumours, PLATINUM METALS REVIEW. (1971) 42--51. http://citeseerx.ist.psu.edu/viewdoc/summary?doi=10.1.1.621.4487 (accessed January 5, 2021).

[167] B. Rosenberg, L. van Camp, T. Krigas, Inhibition of cell division in Escherichia coli by electrolysis products from a platinum electrode [17], Nature. 205 (1965) 698–699. https://doi.org/10.1038/205698a0.

[168] J.P. Macquet, T. Theophanides, DNA-platinum interactions. Characterization of solid DNAK2[PtCl4 complexes, Inorganica Chimica Acta. 18 (1976) 189–194. https://doi.org/10.1016/S0020-1693(00)95602-0.

[169] N. Donaldson, C. Lamont, A. Shah Idil, M. Mentink, T. Perkins, Apparatus to investigate the insulation impedance and accelerated life-testing of neural interfaces, (2018). https://doi.org/10.1088/1741-2552/aadeac.

[170] A. Lasia, Electrochemical impedance spectroscopy and its applications, Kluwer Academic/Plenum Publishers, 1999. https://doi.org/10.1007/978-1-4614-8933-7.

[171] R. Ehret, W. Baumann, M. Brischwein, A. Schwinde, K. Stegbauer, B. Wolf, Monitoring of cellular behaviour by impedance measurements on interdigitated electrode structures, Biosensors and Bioelectronics. 12 (1997) 29–41. https://doi.org/10.1016/0956-5663(96)89087-7.

[172] C. Newbold, R. Richardson, R. Millard, P. Seligman, R. Cowan, R. Shepherd, Electrical stimulation causes rapid changes in electrode impedance of cell-covered electrodes, Journal of Neural Engineering. 8 (2011) 036029. https://doi.org/10.1088/1741-2560/8/3/036029.

[173] T. Geninatti, G. Bruno, B. Barile, R.L. Hood, M. Farina, J. Schmulen, G. Canavese, A. Grattoni, A. Org, Impedance characterization, degradation, and in vitro biocompatibility for platinum electrodes on BioMEMS, Biomed Microdevices. 17 (2015) 24. https://doi.org/10.1007/s10544-014-9909-6.

[174] X. Qian, N. Gu, Z. Cheng, X. Yang, E. Wang, S. Dong, Methods to study the ionic conductivity of polymeric electrolytes using a.c. impedance spectroscopy, Journal of Solid State Electrochemistry. 6 (2001) 8–15. https://doi.org/10.1007/s100080000190.

[175] D.A. Koutsouras, P. Gkoupidenis, C. Stolz, V. Subramanian, G.G. Malliaras, D.C. Martin, Impedance Spectroscopy of Spin-Cast and Electrochemically Deposited PEDOT:PSS Films on

Microfabricated Electrodes with Various Areas, ChemElectroChem. 4 (2017) 2321–2327. https://doi.org/10.1002/celc.201700297.

[176] P.A. Cody, J.R. Eles, C.F. Lagenaur, T.D.Y. Kozai, X.T. Cui, Unique electrophysiological and impedance signatures between encapsulation types: An analysis of biological Utah array failure and benefit of a biomimetic coating in a rat model HHS Public Access, Biomaterials. 161 (2018) 117–128. https://doi.org/10.1016/j.biomaterials.2018.01.025.

[177] T.D.Y. Kozai, K. Catt, X. Li, Z. v. Gugel, V.T. Olafsson, A.L. Vazquez, X.T. Cui, Mechanical failure modes of chronically implanted planar silicon-based neural probes for laminar recording, Biomaterials. 37 (2015) 25–39. https://doi.org/10.1016/j.biomaterials.2014.10.040.

[178] J.A. Last, P. Russell, P.F. Nealey, C.J. Murphy, The applications of atomic force microscopy to vision science, Investigative Ophthalmology and Visual Science. 51 (2010) 6083–6094. https://doi.org/10.1167/iovs.10-5470.

[179] M.J. Walzak, R. Davidson, M. Biesinger, The Use of XPS, FTIR, SEM/EDX, Contact Angle, and AFM in the Characterization of Coatings, Journal of Materials Engineering and Performance. 7 (1998) 317–323. https://doi.org/10.1361/105994998770347747.

[180] T. Tong, B. Babatope, S. Admassie, J. Meng, O. Akwogu, W. Akande, W.O. Soboyejo, Adhesion in organic electronic structures, Journal of Applied Physics. 106 (2009) 083708. https://doi.org/10.1063/1.3246786.

[181] K. Rokosz, T. Hryniewicz, D. Matỳsek, S. Raaen, J. Valíček, Ł. Dudek, M. Harničárová, SEM, EDS and XPS analysis of the coatings obtained on titanium after plasma electrolytic oxidation in electrolytes containing copper nitrate, Materials. 9 (2016). https://doi.org/10.3390/ma9050318.

[182] S.F. Cogan, A.A. Guzelian, W.F. Agnew, T.G.H. Yuen, D.B. McCreery, Over-pulsing degrades activated iridium oxide films used for intracortical neural stimulation, Journal of Neuroscience Methods. 137 (2004) 141–150. https://doi.org/10.1016/j.jneumeth.2004.02.019.

[183] A. Inoue, H. Yuk, B. Lu, X. Zhao, Strong adhesion of wet conducting polymers on diverse substrates, Science Advances. 6 (2020) eaay5394. https://doi.org/10.1126/sciadv.aay5394.

[184] K.W. Vogt, P.A. Kohl, W.B. Carter, R.A. Bell, L.A. Bottomley, Characterization of thin titanium oxide adhesion layers on gold: resistivity, morphology, and composition, Surface Science. 301 (1994) 203–213. https://doi.org/10.1016/0039-6028(94)91300-5.

[185] J. Qu, N. Garabedian, D.L. Burris, D.C. Martin, Durability of Poly(3,4-ethylenedioxythiophene) (PEDOT) films on metallic substrates for bioelectronics and the dominant role of relative shear strength, Journal of the Mechanical Behavior of Biomedical Materials. 100 (2019) 103376. https://doi.org/10.1016/j.jmbbm.2019.103376.

[186] H. Tang, B. Foran, D.C. Martin, Quantitative measurement of adhesion between polypropylene blends and paints by tensile mechanical testing, Polymer Engineering & Science. 41 (2001) 440–448. https://doi.org/10.1002/pen.10741.

[187] C. Girardeaux, E. Druet, P. Demoncy, M. Delamar, The polyimide (PMDA-ODA) titanium interface. Part 2. XPS study of polyimide treatments and ageing, Journal of Electron

Spectroscopy and Related Phenomena. 74 (1995) 57–66. https://doi.org/10.1016/0368-2048(95)02351-8.

[188] F.D. EGITTO, L.J. MATIENZO, K.J. BLACKWELL, A.R. KNOLL, Oxygen plasma modification of polyimide webs: effect of ion bombardment on metal adhesion, Journal of Adhesion Science and Technology. 8 (1994) 411–433. https://doi.org/10.1163/156856194X00311.

[189] D. Ham, J. Lee, Transition Metal Carbides and Nitrides as Electrode Materials for Low Temperature Fuel Cells, Energies. 2 (2009) 873–899. https://doi.org/10.3390/en20400873.

[190] S. Seok, H. Park, J. Kim, Characterization and Analysis of Metal Adhesion to Parylene Polymer Substrate Using Scotch Tape Test for Peripheral Neural Probe, Micromachines 2020, Vol. 11, Page 605. 11 (2020) 605. https://doi.org/10.3390/MI11060605.

[191] V. Radun, R.P. von Metzen, T. Stieglitz, V. Bucher, A. Stett, Evaluation of adhesion promoters for Parylene C on gold metallization, Current Directions in Biomedical Engineering. 1 (2015) 493–497. https://doi.org/10.1515/cdbme-2015-0118.

[192] C. Hassler, R.P. von Metzen, P. Ruther, T. Stieglitz, Characterization of parylene C as an encapsulation material for implanted neural prostheses, Journal of Biomedical Materials Research Part B: Applied Biomaterials. 9999B (2010) NA-NA. https://doi.org/10.1002/jbm.b.31584.

[193] D. Zeniieh, A. Bajwa, L. Ledernez, G. Urban, Effect of Plasma Treatments and Plasma-Polymerized Films on the Adhesion of Parylene-C to Substrates, Plasma Processes and Polymers. 10 (2013) 1081–1089. https://doi.org/10.1002/ppap.201300045.

[194] C. Boehler, F. Oberueber, T. Stieglitz, M. Asplund, Nanostructured platinum as an electrochemically and mechanically stable electrode coating, in: Proceedings of the Annual International Conference of the IEEE Engineering in Medicine and Biology Society, EMBS, Institute of Electrical and Electronics Engineers Inc., 2017: pp. 1058–1061. https://doi.org/10.1109/EMBC.2017.8037009.

[195] L. Ouyang, B. Wei, C. chen Kuo, S. Pathak, B. Farrell, D.C. Martin, Enhanced PEDOT adhesion on solid substrates with electrografted P(EDOT-NH2), Science Advances. 3 (2017) e1600448. https://doi.org/10.1126/sciadv.1600448.